# Contribution of eukaryotic initiation factors (eIFs) to gliomagenesis

**Master thesis**

submitted in accordance with the requirements for the degree of a

**MASTER OF SCIENCE (M.Sc)**

of the Graz University of Technology

Supervisor
Assoz. Prof. Dr. Dr. Johannes Haybäck
Translational Medical Research Group
Institute of Pathology
Medical University Graz

presented by
Christina Ernst, B.Sc.
Graz, January 2013

# STATUTORY DECLARATION

I declare that I have authored this thesis independently, that I have not used other than the declared sources / resources, and that I have explicitly marked all material which has been quoted either literally or by content from the used sources.

Graz, 14. 01. 2013

(date)

(Signature)

# Table of content

# 1   Abstract

Glioblastoma (GBM) is one of the most aggressive primary brain tumor entities in adults. The median survival time of GBM patients is in the range of 14 months and cannot be sufficiently prolonged with currently available therapies.

Protein synthesis is mainly regulated at the rate limiting step of translation initiation which is monitored by eukaryotic initiation factors (eIFs). Deregulation of eIFs may lead to malignant transformation through uncontrolled cell growth. Their mode of action is linked to mTOR signaling.

By performing histological and immunohistochemical stainings, Western Blot and real-time RT-PCR analysis, cell culture experiments and analyzing already existing oligo microarray tumor data sets of astrocytomas of WHO grade I - IV, we were able to draw an expression pattern for specific eIFs and members of the mTOR pathway cascade.

The here presented findings will be the basis for further research with the aim of understanding the role of eIFs in GBM formation and glioma progression in order to design new therapies with the aim of prolonging the life span of GBM patients.

## 2 Zusammenfassung

Glioblastome (GBM) zählen zu den aggressivsten primären Hirntumoren im Erwachsenenalter. Die durchschnittliche Lebenserwartung von 14 Monaten kann mit der heutzutage verwendeten Standardtherapie nicht wesentlich verlängert werden.

Die Synthese von Proteinen wird hauptsächlich zum Zeitpunkt der Translations-Initiation reguliert, überwacht von den eukaryotischen Initiationsfaktoren (eIFs). Dieser Schritt bestimmt somit vorrangig die Translationsrate. Eine Deregulation dieser Initiationsfaktoren kann zu unkontrolliertem Zellwachstum und folglich zur Entstehung von Tumoren führen. Die Funktion der eIFs kann zudem auch mit der mTOR-Signalkaskade in Verbindung gebracht werden.

Mittels histologischer und immunhistochemischer Färbungen, Western Blot- und real-time RT-PCR-Analysen, Zellkulturexperimenten und durch Auswertung bestehender Oligo-Microarray-Daten von WHO Grad I – IV Astrozytomen, war es uns möglich, ein Expressionsprofil spezifischer eIFs und Mitgliedern des mTOR-Signalweges zu erstellen.

Die hier dargestellten Ergebnisse stellen die Grundlage für weiterführende Experimente dar, mit dem Ziel die Rolle der eIFs bei der Entstehung von GBMs zu ergründen und neue Therapiemöglichkeiten zur Verlängerung der Lebenserwartung von GBM-Patienten zu entwickeln.

# 3    Introduction

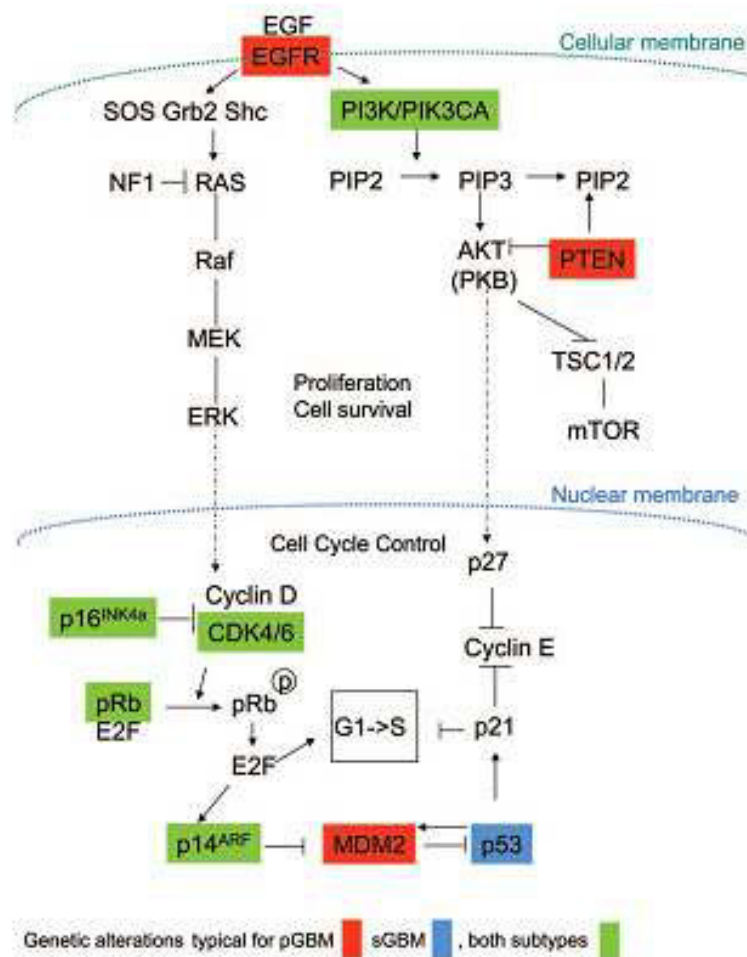## 3.1    Gliomas

Gliomas are the most common primary brain tumor entity in adults and are among the most malignant of all cancer types. The median survival time after initial diagnosis is about 14 months and until now cannot be prolonged considerably with currently available therapies[1,2]. Clinical symptoms depend primarily upon the site of tumor location. Most often the tumor is located in the cerebral hemispheres, less frequently in the brain stem, cerebellum or spinal cord. Gliomas originate from glial cells in the brain through acquisition of genetic alterations, in particular deregulation of oncogenes, tumor suppressor genes and genes involved in signal transduction and cell cycle regulation[3,4]. According to the World Health Organization (WHO) gliomas can be classified as grade I-IV tumors[5]. WHO grade II-IV [II. diffuse astrocytoma, oligodendroglioma; III. anaplastic astrocytoma, anaplastic oligodendroglioma; IV. glioblastoma (glioblastoma multiforme, GBM)] tumors display a diffuse infiltrative growth pattern, which is responsible for the high recurrence rate after surgical resection of the tumor, while grade I (pilocytic astrocytoma) astrocytomas may frequently be surgically cured. Approximately half of the diagnosed gliomas are GBMs, which is the most aggressive form of these brain intrinsic tumors, classified as WHO grade IV. In Europe, the incidence is in the range of 2 – 3 cases per 100 000 people[6]. GBM may develop *de novo* (primary) or from low-grade astrocytomas or oligodendrogliomas (secondary). Primary GBMs typically develop in older patients (mean 62 years). They manifest very rapidly and patients usually have a shorter clinical history. Secondary GBMs occur less frequent than primary subtype and most commonly affect younger patients (mean 45 years)[7]. Histologically, GBMs are characterized by poorly differentiated, highly pleomorphic astrocytic tumor cells with nuclear atypia and high mitotic activity. Typical hallmark features are band-like necrosis and microvascular (glomeruloid endothelial) proliferations. Some GBMs usually display a high degree of cellular and nuclear pleomorphism and high numbers of mitotically active cells, sometimes intermixed with numerous multinucleated giant tumor cells[3].

### 3.1.1    Molecular background

Gliomagenesis is a multistep process involving the sequential acquisition of genetic alterations. Primary and secondary GBMs have been shown to be relative distinct disease

entities which evolve through different genetic pathways and thereby show different expression profiles[8]. This difference might be explained by a higher degree of genomic instability in primary tumors[5]. Both subtypes show high frequency of loss of heterozygosity (LOH) in chromosome 10q, which in turn is the most frequent genetic alteration in GBM at all (80%). Other prominent abnormalities are *EGFR* amplification or overexpression (~40%), *PTEN* mutation (15 – 40%), *MDM2* amplification or overexpression (~50%) in primary GBM and *TP53* mutation, which is most common in secondary GBM (>65%). Also loss of p14$^{ARF}$ expression (76%) and inactivation of genes in the p16$^{INK4a}$/CDK4/RB1 pathway are found in both GBM subtypes (Figure 1). Mutations in *IDH1* are typically seen in astrocytomas of grade II and III[2,5,8].



**Figure 1 Major signaling pathways involved in gliomagenesis.** The CDK/cyclin/CDK inhibitor/RB, the p53 and the RTK/RAS/PI3K pathway are the most prominent pathways affected in the formation of malignant gliomas. Genetic alterations typical for primary and secondary GBMs or both subtypes are highlighted in red, blue and green, respectively (Modified from Ohgaki et al., 2007[9]).

In 2008 "The Cancer Genome Atlas" (TCGA) Research Network made a large-scale gene expression profile study including 206 patient GBM samples in order to generate a catalogue of genomic abnormalities driving tumorigenesis[10]. They were able to describe three core pathways potentially involved in GBMs: The CDK/cyclin/CDK inhibitor/RB pathway important for cell division; the p53 pathway, which regulates the response to DNA damage and cell death; and the RTK/RAS/PI3K pathway, which is involved in the regulation of growth factor signals (Figure 1). Hereupon, Verhaak et al. used the full scope of TCGA data to design four molecular subtypes of GBM based on combinations of over- and underexpressed genes via consensus clustering[11]. The subtypes were called classical, mesenchymal, proneural and neural (Figure 2). The classical subtype comprises highly proliferative cells and is characterized by *EGFR* amplification and loss of *PTEN* and *CDKN2A* gene loci as a result of gains on chromosome 7 and losses on chromosome 10 and 9p21.3. The mesenchymal subtype frequently shows inactivation of the *NF1, TP53* and *PTEN* genes. The proneural subtype is associated with better survival, as compared to the other subtypes. The
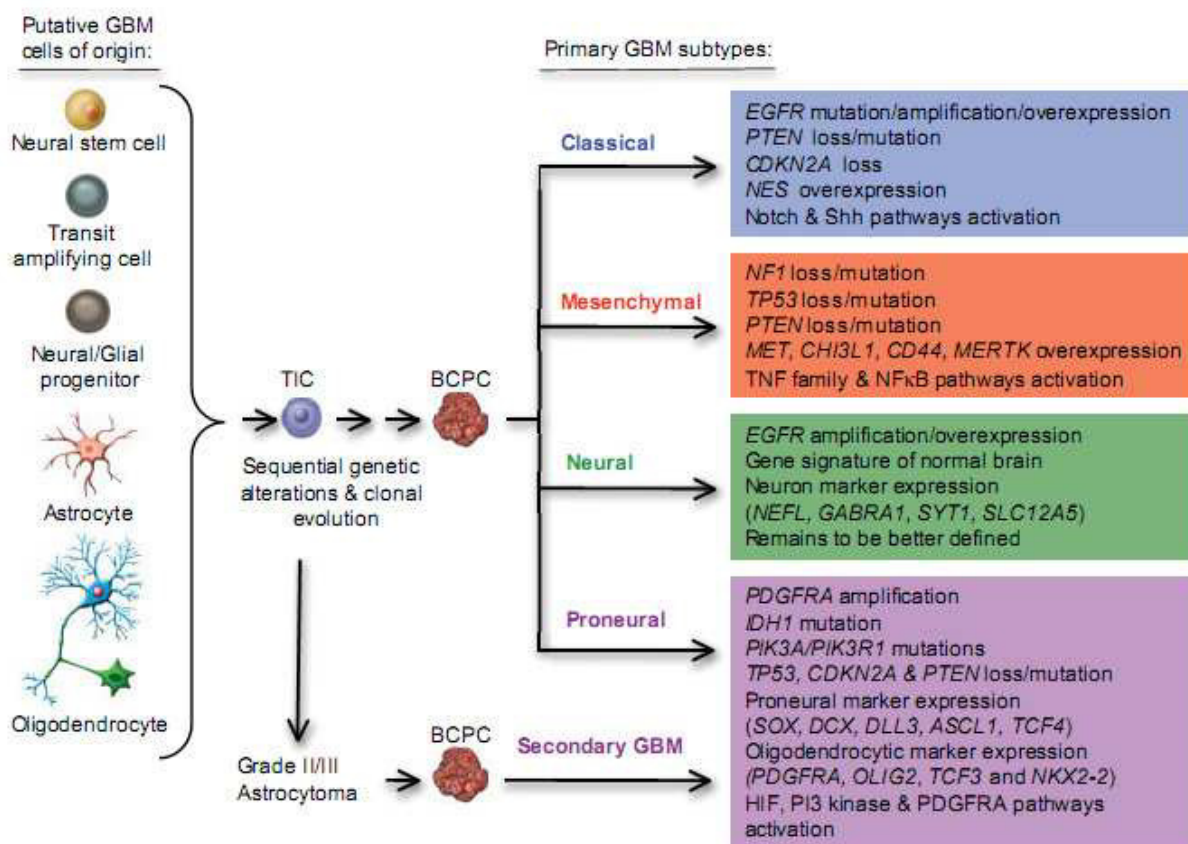


**Figure 2 Molecular subtypes of glioblastoma.** GBMs develop from different cells of origin through the sequential acquisition of genetic alterations involving cell signaling and cell cycle regulation pathways. Based on varying combinations of genetic changes four molecular subtypes can be distinguished. TIC, tumor-initiating cells; BCPC, brain cancer-propagating cells (Modified from Van Meir et al.[4]).

expression profile includes overexpression/amplification of *PDGFRA* and mutations in *IDH1, TP53* and *PIK3CA/PIK3R1.* The neural GBM subtype has a gene expression similar to normal brain tissue[4,11]. The different expression profiles of these four subtypes might help to select more specific therapies for each group and might be used to predict patient outcome and response to treatment.

### 3.1.2 Therapy strategies

Currently available therapies for GBM treatment are surgical resection followed by radiation and chemotherapy[12,13]. The use of the fluorescent tumor marker 5-aminolevulinic acid (5-ALA) for intraoperative guidance helps to maximize surgical resection of the tumor and improves survival of the patient[4]. Following surgery, a combination of radiotherapy and treatment with the alkylating agent temozolomide is at present the most effective strategy to improve survival of the patients, compared to radio- or chemotherapy alone[2]. Unraveling the molecular signature of gliomas has led to the development of new molecular drugs specifically targeting altered growth factor and angiogenesis pathways and intracellular pathways downstream of both. The RTK/PI3K/Akt/mTOR pathway seems to be the most amenable target to pharmacological intervention (Figure 3)[14]. Several small molecule inhibitors, monoclonal antibodies or gene therapy approaches have been and currently are tested in clinical trials, however, with rather disappointing results. To date, none of the attempts in inhibiting EGFR, PDGFR, or VEGF, as well as PI3K, Akt and mTOR could prolong patient survival[15–17]. Due to insufficient single-agent activity of such inhibitors a combination with standard therapy or concurrent inhibition of multiple targets might bring an additional benefit to the patient. In this case, an increased risk of toxic effects from systemic administration has to be considered.

Resistance to therapy can be ascribed to a variety of factors. First of all, malignant gliomas are highly heterogeneous tumors that evolve through a multi-step process involving several genes and signaling pathways. Also, primary and secondary GBMs show different molecular profiles, all leading to different sensitivities to targeted therapies. Next, increased expression of $O^6$-methylguanine-DNA methyltransferase (MGMT), a DNA repair enzyme, is capable of reversing the effect of alkylating agents, such as temozolomide[18]. In addition to that, the existence of glioma stem-like cells (GSCs) within the tumor contributes to therapy failure. GSCs have stem cell properties and are able to undergo self-renewal and initiate tumorigenesis. This makes them resistant to a variety of chemotherapeutic agents and

radiation and allows them to assist in tumor maintenance[19]. Another factor limiting the efficacy of anticancer drugs is insufficient penetration into the tumor tissue due to the blood-brain-barrier. Here, local therapies such as implantation of drug containing wafers might help to overcome resistance[14].

Despite the advances in therapeutic approaches prognosis is still very poor and the tumor is either insensitive to therapy or rapidly develops resistance. Thus an even better molecular understanding of gliomagenesis, genetic alterations and gene expression changes underlying glioma formation is essential to design new treatment strategies.
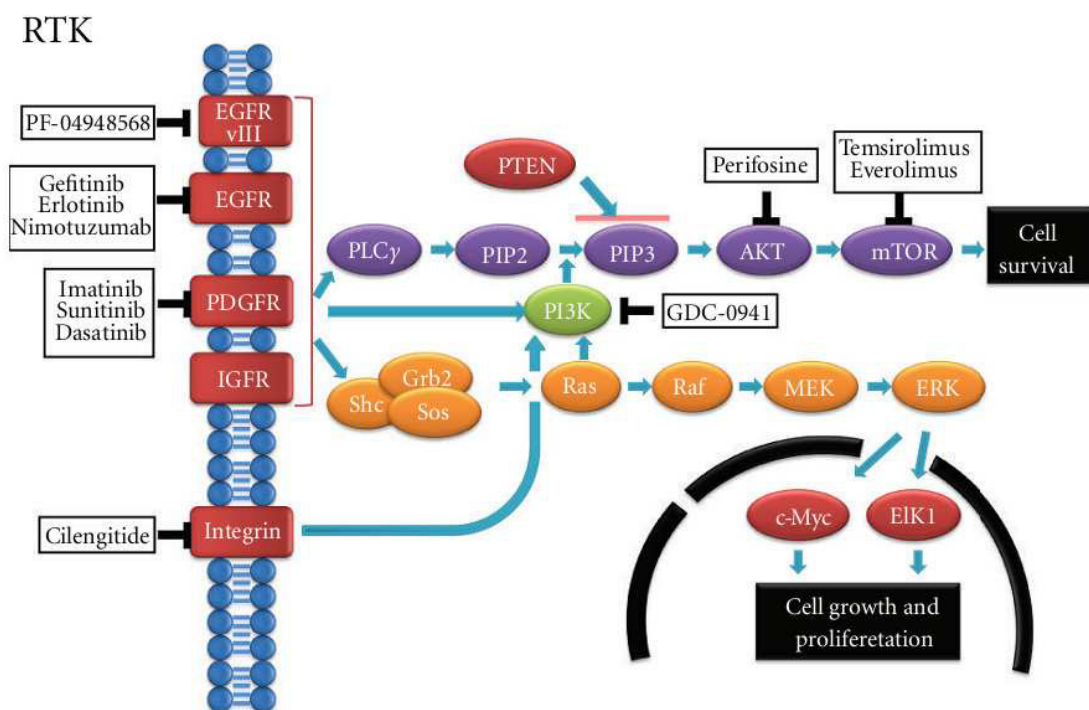


**Figure 3 Altered signaling pathways in GBM and inhibitors.** Several members of the RTK signaling pathway have already been targeted with specific molecular agents. The results of most clinical studies are, however, disappointing (Modified from Ohka et al. [14]).

## 3.2   Translation initiation

Protein synthesis is a complex process and can be divided into several parts, one of it being mRNA translation. Translation is a highly regulated process and can be divided into 4 steps: initiation, elongation, termination and ribosome recycling. Regulation is mainly executed at the initiation step, which is often referred to as the rate-limiting step. Dysregulation of

mRNA translation leads to abnormal gene expression and thus can result in cancer formation through uncontrolled cell growth[20].

Translation initiation can again be divided into several steps which are monitored by eukaryotic initiation factors, eIFs. Currently 12 core eIFs are known: eIF1, eIF1a, eIF2, eIF2b, eIF3, eIF4a, eIF4e, eIF4g, eIF4b, eIF4h, eIF5 and eIF5b and the non-core eIF6[20,21]. The first step of translation initiation is the formation of the 43S ribosome pre-initiation complex (Figure 4). It consists of the small 40S ribosomal subunit, the initiating methionyl-tRNA (Met-tRNAi) and a group of eIFs, including eIF2 and eIF3. This complex recognizes, together with eIF3 and the 4F complex, the 5' cap structure of the mRNA and binds to it. The eIF4F complex comprises the scaffold protein eIF4g, the helicase eIF4a and the cap-binding protein eIF4e, which specifically recognizes the 7-methyl guanosine cap (m7G cap) of the mRNA[22]. When bound to the mRNA, the complex scans the 5' UTR until it finds the correct start
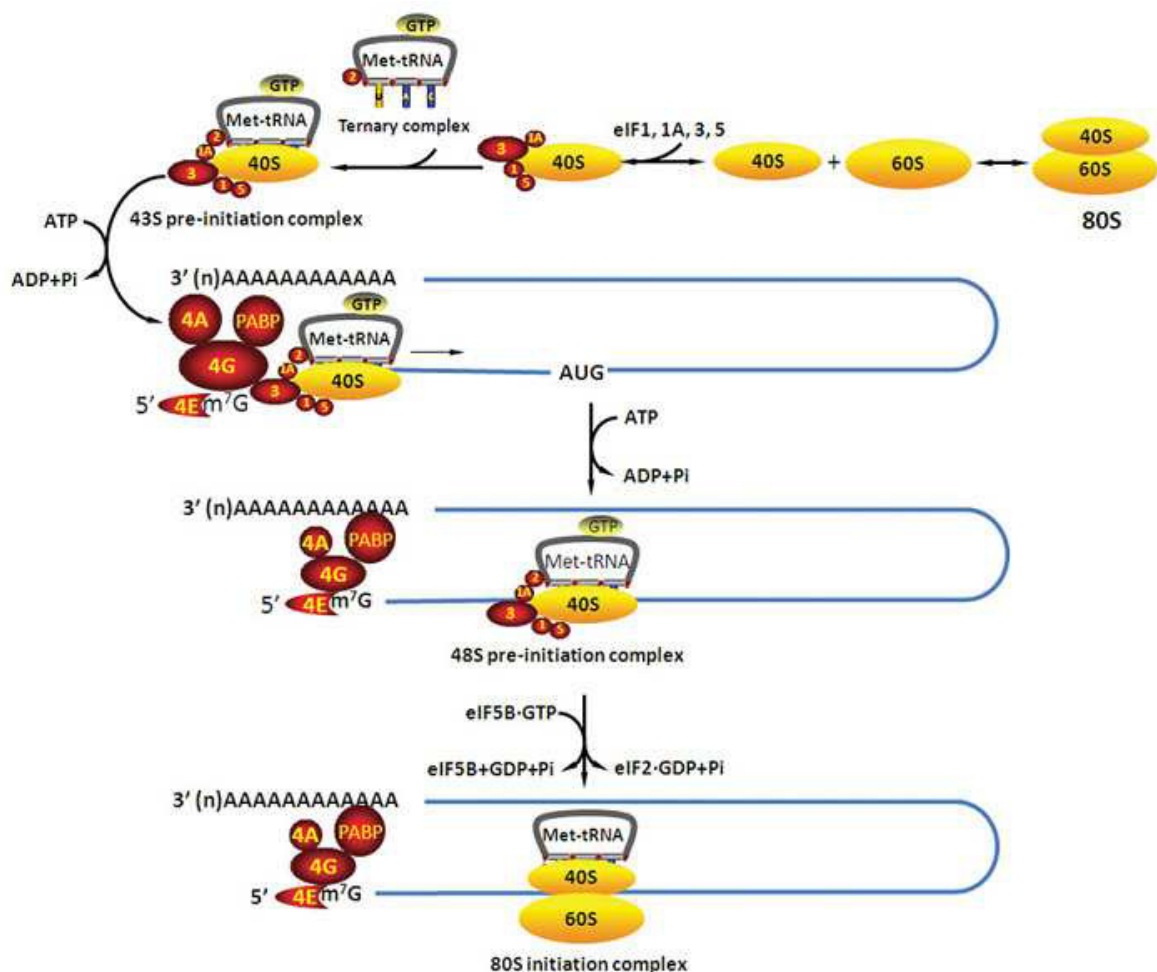


**Figure 4 Translation initiation and eIFs.** Translation initiation comprises a number of steps which are monitored by different eIF subunits. They assist in 5' cap recognition, 5'UTR scanning, start codon (ATG) recognition and the onset of elongation by formation of the functional 80S ribosome (Modified from Yin et al.**[32]**).

codon. Recognition of AUG leads to the association of eIF5 followed by the hydrolysis of eIF2-bound GTP molecules, resulting in recruitment of the 60S ribosomal subunit. The endpoint of this initiation process is the formation of the functional 80S ribosome attached to the mRNA and the release of the eIFs from the ribosome. The next step in the cascade is the onset of elongation [23,24].

eIFs have been shown to be linked to mTOR signaling and cell cycle regulation and they may serve as tumor suppressors or promote carcinogenesis and tumor progression in different types of cancer[25]. As an example, eIF3a, which is the largest subunit of the eIF3 complex, is upregulated in breast, cervical, colon, lung and stomach cancer[26–31]. Knocking down eIF3a expression reversed the malignant phenotype of human lung and breast cancer cell lines[32]. Knockdown of eIF3b was recently shown to significantly inhibit the proliferation of human GBM cells (U87)[33]. eIF4e, which is strongly linked to the mTOR signaling cascade, is associated with decreased survival in breast cancer patients and was shown to be
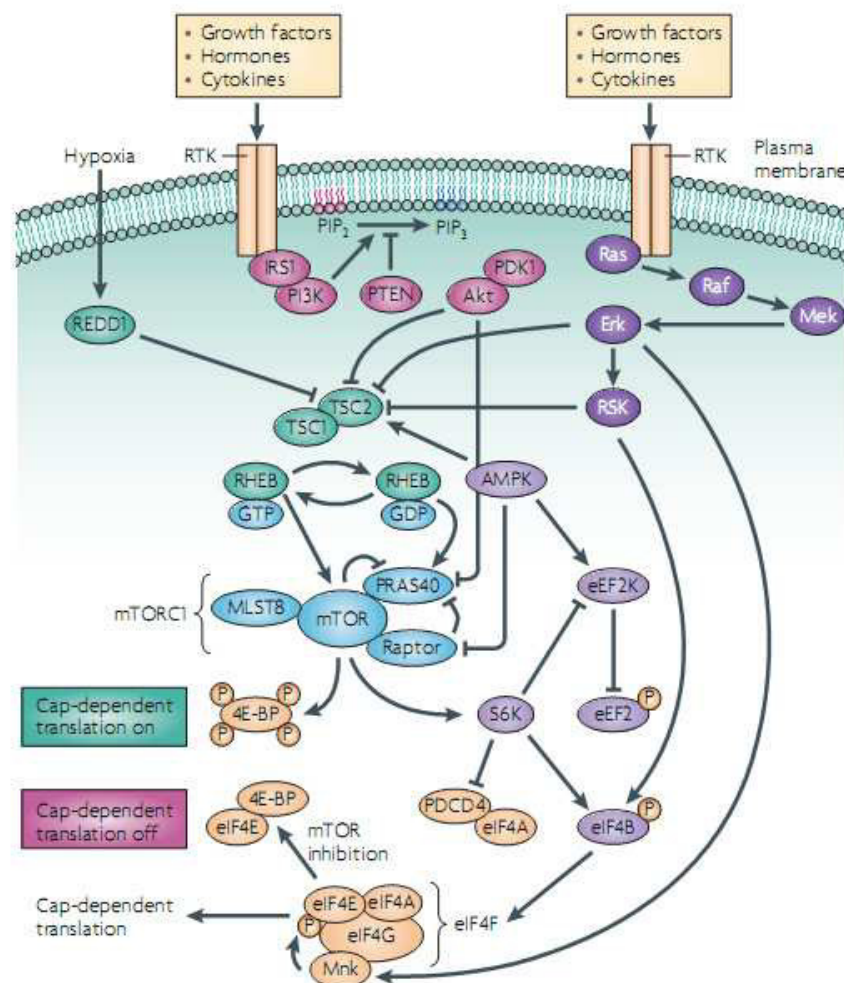


**Figure 5 RTK signaling and translation initiation.** (Modified from Silvera et al.[21])

9

upregulated in colorectal, ovarian and lung cancer, astrocytic tumors and other cancers[34–38].

The RTK/PI3K/mTOR signaling pathway is critical in mRNA translation and plays a pivotal role in cell growth and survival. It functions by integrating mitotic signals to control translation rates[39]. Binding of mitotic signals to receptor tyrosine kinases (RTKs) on the cell surface triggers an intracellular signal cascade leading to the activation of Akt and mTOR. In parallel, the Ras/Erk/MAPK pathway can be activated. Many components of this pathways have been shown to be either mutated or amplified in human cancers, such as GBM, lung, breast and endometrial cancer and thus represent important targets in cancer therapeutics[40–43]. Two downstream targets of mTOR are p70S6K and the eIF4E-binding protein 1 (4E-BP1). The translational repressor 4E-BP1 binds eIF4e, prevents its interaction with the eIF4F complex and consequently inhibits cap-dependent translation initiation[39]. When 4E-BP1 is phosphorylated by mTOR, eIF4e gets released and is able to promote translation (Figure 5). The second mTOR target p70S6K, when activated, phosphorylates eIF4b, increasing its association with eIF4a. Further, it phosphorylates programmed cell death protein 4 (PDCD4), blocking its inactivation of eIF4a[21]. Activated Erk promotes phosphorylation of eIF4b through RSK, which in turn triggers mRNA binding of the eIF4F complex (Figure 5). This again leads to enhancement of translation initiation[21].

### 3.2.1 Therapeutic options

Since eIFs are key factors in regulating cellular homeostasis and deregulation might promote malignant transformation leading to tumorigenesis, they are attractive targets for cancer therapy. Of the different eIFs, eIF4e is the most extensively targeted member so far[44]. One reasonable approach is to disrupt the cap-binding activity of eIF4e with cap-analogs, such as 4Ei-1 or the anti-viral drug ribavirin[45,46]. They mimic the 5'-cap of the mRNA and thereby inhibit its interaction with eIF4e. Another potential therapeutic compound that has shown promising results in pre- and clinical trials is the specific anti-sense oligonucleotide 4E-ASO, suppressing eIF4e on a genetic level[47]. Further, being a downstream target of mTOR, different studies aim to indirectly target eIF4e with mTOR inhibitors. Rapamycin and related drugs (rapalogs) block mTOR driven phosphorylation of 4E-BPs and consequently inhibit the translation initiation potential of eIF4e. However, additional clinical trials are needed to evaluate the efficacy and the safety of such drugs as single agents as well as in combination with standard therapies[44].

## 3.3   Aim of the study

In this project our aim was to investigate the contribution of eIFs in glioma development and link eIF expression patterns to mTOR signaling. Understanding the role of eIFs in GBM formation and progression might lead to the development of novel therapeutic approaches in addition to surgical resection, radiation and the so far established chemotherapy with the aim of prolonging the life span of glioma patients.

# 4    Materials and Methods

## 4.1    Cell culture

The glioblastoma cell lines U87MG and U251, as well as the HeLa cell line, were received from the Medical University of Graz and the Center for Medical Resarch Graz, respectively. The cell lines U118, U373 and U1242, as well as the primary GBM cell cultures KW1, KDW2, Pat4 and Pat8 were kindly provided by the Experimental Pharmacology & Oncology Berlin-Buch GmbH (EPO Berlin). The glioblastoma cells were grown in culture flasks in DMEM [High Glucose, Pyruvate (Gibco)], HeLa cells in MEM (Gibco), supplemented with 10% fetal bovine serum (FBS) and 1% penicillin/streptomycin. The primary cell cultures were kept in MEM (GibcO), supplemented with 10% fetal bovine serum (FBS), 1% penicillin/streptomycin and 1X MEM Non-essential amino acids (Gibco). Cells were cultured at a temperature of 37°C, a relative humidity of 95% and an atmosphere of 5% $CO_2$.

For protein extraction, cells were cultured on Petri Culture Dishes (100 mm x 20 mm), washed with PBS three times, harvested with a cell scraper in 1 ml PBS and collected through centrifugation at 10 000 rpm at 4°C for 10 minutes. The supernatant was discarded and the cell pellets stored at -80°C until further usage.

## 4.2    Tumor samples

Patient samples were supplied from the Departments of Neurosurgery and Neuropathology at the Medical University of Graz (Austria). Brain tumors that were routinely resected and histologically characterized according to WHO classifications[5] were collected and analyzed. The tissue samples were shock frozen in liquid nitrogen immediately after surgery and stored at -80°C.

Tissue specimens were registered in the biobank and kept anonymous. The research project was authorized by the ethical committee of Graz (Ek-Nr. 24-143 ex 11/12). The study protocol was in accordance with the ethical guidelines of the Helsinki declaration. Patients were enrolled after giving their written informed consent.

## 4.3    Protein analysis

### 4.3.1    Protein isolation

Total protein was isolated from 2 normal brain tissues, 3 grade I – IV glioma samples, respectively, and all cell lines and primary GBM cells.

For the isolation of protein from tissue samples, frozen brain tissue was homogenized with 300 – 500 µl of NP-40 Lysis buffer using MagNA Lyser Green Beads (Roche) for 30 seconds at 6500 rpm with the MagNA Lyser (Roche). Cell culture pellets were homogenized using a Potter tissue homogenizer. The lysate was transferred into a new tube and centrifuged at 10 000 rpm for 10 minutes at 4°C. The supernatant was again transferred into a fresh tube. Protein concentration was determined using the Bradford protein assay and adjusted to 6 µg/µl with SDS-Sample Buffer. The samples were stored at -80°C until further usage.

| **NP-40 Lysis Buffer** | 1M Tris HCl (pH 7.5) | 25 ml |
|---|---|---|
| | 5M NaCl | 15 ml |
| | NP-40 | 2.5 ml |
| | ddH$_2$O | ad 500 ml |

Freshly added:

1 tablet of Complete Mini and PhosSTOP, dissolved in 1 ml ddH$_2$O

| 0.1 M Pefabloc | 100 µl |
|---|---|
| 1 M DTT | 10 µl |
| NP-40 Lysis buffer | 9 ml |

### 4.3.2 Determination of protein concentration

Protein concentration was measured using the Bradford protein assay. A BSA standard curve was made using following concentrations: 0.5, 1, 2, 4, 6, 8, 10 µg/µl. For measurement, the Bradford solution (Bio-Rad) was diluted 1:5 with Aqua dest. 998µl of the diluted solution were transferred into cuvettes and 2 µl of protein sample were added. At too high protein concentrations, the samples were diluted 1:5 in Aqua dest. prior to addition. The samples were mixed well, incubated for 15 minutes and measured with a photometer (BioPhotometer plus, Eppendorf) at 594 nm. All samples were measured in a triplicate. Protein concentrations were calculated according to the BSA standard curve.

### 4.3.3 SDS-PAGE and Western Blot

Protein samples were separated according to their molecular mass by SDS-PAGE and transferred onto a membrane for immunodetection. For SDS-PAGE, 8% or 12.5% gels were casted in consideration of the molecular mass of the protein of interest. The samples were

prepared with SDS Sample Buffer (Bio-Rad) as mentioned above and heated for 5 minutes at 95°C. A total protein amount of 60 µg was loaded on the gel and electrophoresis was performed for 1.5 h at 120 V in 1x SDS Running Buffer with the Mini-vertical electrophoresis unit (Amersham Biosciences). As a molecular weight marker the Novex Sharp Pre-Stained Protein Standard (4 µl) was used. Next, the separated proteins were transferred onto a PVDF-membrane (Immobilin-P Transfer Membran; Millipore) using a Semi Dry Blotting Unit (JH BioInnovations) at 160 mA for 1.5 hours. Prior to the electrotransfer the membrane was activated by rinsing it 15 seconds with Methanol, 2 minutes with aqua dest. and 5 minutes with Towbin Transfer Buffer. Successful transfer was checked for by Ponceau Red staining.

For immunodetection, the membrane was blocked in 5% nonfat dried milk powder (Applied Chemistry) in TBS-Tween (0.1%) for 1 hour. Then, the membrane was washed 3 times for 5 minutes with TBS-Tween (0.1%) and incubated with the primary antibody (diluted according to manufacturer's instructions) overnight at 4°C, agitating. The following day, the membrane was again washed 3 times with TBS-Tween (0.1%) for 5 minutes and incubated with the secondary antibody solution (Anti-rabbit; Amersham, 1/5000). Detection was performed using the ECL Plus Western Blotting Detection Reagents (GE Healthcare) and exposure to ECL Hyperfilms (GE Healthcare).

| **SDS Running Buffer (10x)** | 250 mM Tris HCl (pH 8.4) | 30.29 g |
| | 192 mM Glycine | 114.13 g |
| | 1% SDS | 10 g |
| | ddH$_2$O | ad 1 l |

| **Towin Transfer Buffer** | 25 mM Tris | 3.03 g |
| | 190 mM Glycine | 14.26 g |
| | 20 % Methanol | 200 ml |
| | ddH$_2$O | ad 1 l |

| **TBS-Tween (10x)** | 0.2 M Tris | 24.2 g |
| | 1.4 M NaCl | 80.0 g |
| | adjust to pH 7.6 with HCl | |
| | ddH$_2$O | ad 1 l |
| | add 0.1% Tween-20 to 1x TBS Buffer | |

| Separation gel | 8% | 10% | 12.5% |
|---|---|---|---|
| AD | 4.6 ml | 4.0 ml | 3.28 ml |
| Tris 1.5 M pH 8.8 | 2.5 ml | 2.5 ml | 2.5 ml |
| Acrylamide | 2.7 ml | 3.3 ml | 4.06 ml |
| 10% SDS | 100 µl | 100 µl | 100 µl |
| APS | 100 µl | 100 µl | 100 µl |
| TEMED | 6 µl | 7.5 µl | 7.5 µl |

**Stacking gel**

| | |
|---|---|
| AD | 3.1 ml |
| Tris 1.5 M pH 6.8 | 1.25 ml |
| Acrylamide | 0.5 ml |
| 10% SDS | 50 µl |
| APS | 25 µl |
| TEMED | 7.5 µl |

**Primary Antibodies**

| | | |
|---|---|---|
| eIF3a | Cell Signaling | 1/1000 |
| eIF3β (A-8) | Santa Cruz | 1/1000 |
| eIF3c | Cell Signaling | 1/1000 |
| eIF3η (D-9) | Santa Cruz | 1/1000 |
| eIF3ζ (H-300) | Santa Cruz | 1/1000 |
| eIF3 p110 (B-6) | Santa Cruz | 1/100 |
| eIF3q (H-300) | Santa Cruz | 1/200 |
| phospho-eIF4b | Cell Signaling | 1/1000 |
| eIF4b | Cell Signaling | 1/1000 |
| eIF4e | Cell Signaling | 1/1000 |
| phospho-4E-BP1 | Cell Signaling | 1/1000 |
| 4E-BP1 | Cell Signaling | 1/1000 |
| Phospho-Akt | Cell Signaling | 1/1000 |
| Akt | Cell Signaling | 1/1000 |
| PTEN | Cell Signaling | 1/1000 |
| mTOR | Cell Signaling | 1/1000 |
| Phospho-p70S6K | Cell Signaling | 1/1000 |
| p70S6K | Cell Signaling | 1/1000 |
| GAPDH | Cell Signaling | 1/3000 |

### 4.3.4 Immunohistochemistry

In total, 78 human glioma samples of WHO grade I – IV, collected at the Medical University of Graz, were examined, including 19 grade I (24.4%), 24 grade II (30.8%), 20 grade III (25.6%) and 15 grade IV tumors (19.2%). Immunohistochemical staining with eIF3a, eIF3 p110 (B-6) and eIF4e antibodies was performed using an automated immunostainer (Ventana BenchMark Ultra). Briefly, formalin-fixed, paraffin embedded tissue sections were deparaffinized, followed by antigen retrieval (CC1 mild). For IHC detection of eIF3a and eIF3 p110 (B-6) the ultraView Universal DAB Detection Kit (Ventana) was used, for eIF4e we used the OptiView DAB IHC Detection Kit (Ventana). Sections were counterstained with haematoxylin.

The pattern of staining was quantified for each individual sample. Intensity was recorded as 0 when there was no detectable labeling, and values of 1, 2, and 3 were used to indicate weak, moderate and strong labeling, respectively. Density scoring was performed in continuous 10%-steps from 0% to 100%. No staining was considered as 0, staining of ≤10% as 1, 11%-49% as 2, 50%-80% as 3 and >80% as 4. For statistical analysis, a total immunostaining score (TIS) was calculated by multiplication of intensity and density score. The data were compared by a nonparametric Mann Whitney U test in R.

### 4.4 Real-time RT-PCR

The gene expression of 5 eIF subunits and 4E-BP1 was analyzed with real-time RT-PCR. Therefore, total RNA was isolated from 5 normal brain samples, 2 gliomas of grade I, 3 gliomas of grade II and III and 6 samples of grade IV gliomas. Total RNA was reverse transcribed into cDNA, which was then subjected to real-time PCR for relative quantification.

### 4.4.1 RNA isolation

Total RNA was isolated from deep-frozen brain tissue using Trizol (Life Technologies). Tissue pieces were homogenized in 1 ml Trizol for 30 seconds at 6500 rpm with the MagNA Lyser (Roche). The lysate was incubated for 10 minutes at RT. Next, 200 µl chloroform was added, mixed, incubated for 3 minutes at RT and centrifuged at 10 000 rpm for 15 minutes at 4°C. The upper phase containing the RNA was carefully transferred into a fresh tube, mixed with 500 µl isopropanol and again centrifuged at 10 000 rpm for 20 minutes at 4°C. The supernatant was discarded and the pellet washed with 1 ml 75% ethanol. The pellet was

then dried at 37°C to completely remove the ethanol and then dissolved in 100 – 200 µl DEPC treated water at 58°C. The RNA samples were stored at -80°C.

### 4.4.2   cDNA synthesis

cDNA was synthesized from total RNA with the High-Capacity cDNA Reverse Transcription Kit (Applied Biosystems) according to the manufacturer's instructions. Short, 20 µg of RNA were mixed with 10 µl of the 2X RT master mix to a total reaction volume of 20 µl. Then, a PCR reaction with the following conditions was performed:

| PCR program | Temperature | Time |
|---|---|---|
| | 25°C | 10 min |
| | 37°C | 120 min |
| | 85°C | 5 min |
| | 4°C | ∞ |

| 2X RT master mix | Component | Volume (µl) | |
|---|---|---|---|
| | 10X RT Buffer | 2.0 µl | |
| | 25X dNTP Mix (100 mM) | 0.8 µl | |
| | 10X RT Random Primers | 2.0 µl | |
| | MultiScribe$^{TM}$ Reverse Transcriptase | 1.0 µl | |
| | RNase Inhibitor | 1.0 µl | |
| | Nuclease-free H$_2$O | 3.2 µl | |
| | **Total per reaction** | **10.0 µl** | **+ 10 µl RNA** |

### 4.4.3   Real-time PCR

Real-time PCR was performed using *Power* SYBR Green PCR Master Mix (Applied Biosystems) according to the recommended protocol. The PCR reaction was made in a final volume of 30 µl containing 5 µl of template cDNA. The primers were designed specific for the different eIF subunits (eIF3a, eIF3c, eIF3j, eIF4b, eIF4e, eIF6) and 4E-BP1.

For relative quantification of the real-time data the ΔΔCt method was used. This method is based on comparing the Ct-value of a sample with a control sample. Here, we compared the Ct-values of tumor samples with the mean Ct-value of the normal brain samples, after normalization to the housekeeping gene GAPDH.

$$\Delta Ct = Ct_{target} - Ct_{reference}$$

$$\Delta\Delta Ct = \Delta Ct_{treated} - \Delta Ct_{control}$$

$$Ratio = 2^{-\Delta\Delta Ct}$$

| Master mix | Component | Volume | |
|---|---|---|---|
| | Power SYBR® Green PCR Master Mix (2X) | 15 µl | |
| | Forward Primer (10 pM) | 1 µl | |
| | Reverse Primer (10 pM) | 1 µl | |
| | Nuclease-free $H_2O$ | 8 µl | |
| | **Total per reaction** | **25 µl** | **+ 5 µl cDNA** |

**Primer sequences**

| Gene | Primer Pair | Sequence (5' –> 3') | Length | Tm (°C) |
|---|---|---|---|---|
| EIF3A | Fwd. | GCCGGAAAATGCCCTCAAAC | 20 | 62,2 |
| | Rev. | TGGTTCGTGTATCTTTTGCCAT | 22 | 60,2 |
| EIF3C | Fwd. | CTGGTCCGGCCGTAGCACCT | 20 | 65,5 |
| | Rev. | CCTCGCTCAGCAACAATGGCTGTT | 24 | 64,4 |
| EIF3J | Fwd. | GTCAAGGATAACTGGGATGACG | 22 | 60,2 |
| | Rev. | CGAGGTCTGACTCTTCCTGTAA | 22 | 60,6 |
| EIF4B | Fwd. | CCTCCCAGTCCACTCGAGCTG | 21 | 65,7 |
| | Rev. | GCTTGGGTGTCTCTCCCGAGG | 21 | 65,7 |
| EIF4E | Fwd. | TGCGGCTGATCTCCAAGTTTG | 21 | 62,9 |
| | Rev. | CCCACATAGGCTCAATACCATC | 22 | 60,0 |
| EIF6 | Fwd. | CCGCGTGCGGAGCTTGTTA | 19 | 61,0 |
| | Rev. | CGCCCTCGAACACACTGTAGAAGT | 24 | 64,4 |
| 4E-BP1 | Fwd. | CACCCCGGGAGGTACCAGGATC | 22 | 67,7 |
| | Rev. | CGCCCGCCCGCTTATCTTCT | 20 | 63,5 |

## 4.5   REMBRANDT Analysis

REMBRANDT (Repository of Molecular Brain Neoplasia Data) is a portal that comprises molecular research and clinical trials data related to brain cancers, including gliomas. It is a joint initiative of the National Cancer Institute (NCI) and the National Institute of Neurological Disorders and Stroke (NINDS) and allows a molecular classification of tumors based on gene expression and genomic data from tumors of patients (National Cancer Institute, 2005. REMBRANDT home page, <http://rembrandt.nci.nih.gov>. Accessed 2010 April 27)[48].

The gene expression profiles of 61 WHO grade II (19.0%), 47 grade III (14.7%) and 191 (59.7%) grade IV gliomas and of 21 non tumors (6.6%) were downloaded, analyzed in R and graphically displayed as box plots[49]. The data was normalized using quantile normalization. Following packages were used in R: affy, annotate, limma and hcu133plus2.db[50–53]. The different eIFs and members of the mTOR signaling cascade were analyzed and compared to the Western Blot data.

# 5 Results

## 5.1 Expression of eIFs in glioma

### 5.1.1 Expression of eiFs in cryo samples of human glioma tissue

The changes in protein expression of different members of the eIF family were analyzed by comparing human astrocytoma samples of WHO grade I - IV with normal brain tissue using Western Blot analysis. The expression pattern of the different eIFs is characterized by evident heterogeneity (Figure 6A). Even within tumors of the same grade huge variations in protein expression were detected. Also relative quantification using ImageJ software revealed high standard deviations in samples of the same tumor entity, exemplified by the diverse expression of eIF3a in grade I and IV astrocytomas. For eIF3q (H-300), eIF3d, eIF3i and eIF4b no clear changes in expression levels between the tumor grades were observed (Figure 6B-J, Table 1). The expression of eIF3a, eIF3b, eIF3c, phospho-eIF4b, and eIF4e was increased in low grade and anaplastic astrocytomas (grade I – III) compared to normal brain tissue and decreases again in GBMs (grade IV).

To evaluate the level of mRNA expression in the tumor samples, real-time RT-PCR was performed. Analogical to the Western Blot data, comparing tumors of grade I – IV to normal brain tissue again revealed an up and down of mRNA expression with the tumor grades (Figure 8A-G). Expression of eIF3a, eIF3c, eIF4b and eIF4e was highest in astrocytomas of grade II and III and lowest in grade IV, whereas eIF3j mRNA levels were highest in grade I tumors. For 4E-BP1 and eIF6 no clear changes were determined.

As for the REMBRANDT data analysis, the most definite changes in mRNA levels were shown for eIF4e, indicating higher mRNA levels for normal brain compared to astrocytomas of grade II-IV. eIF3a and eIF4b mRNA levels are highest in grade II tumors, for eIF3c there were no differences observed (Figure 7A-G).
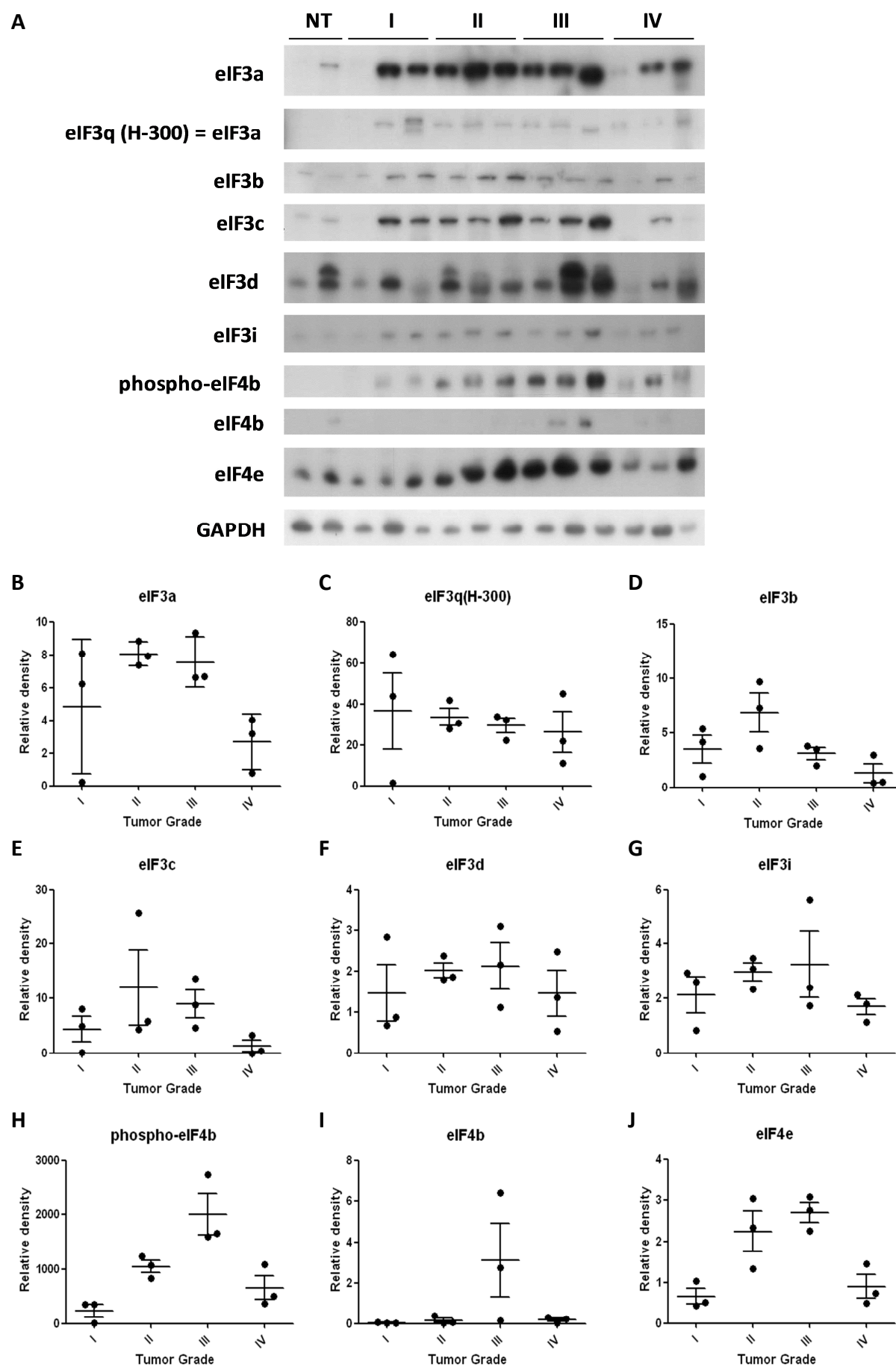
**Figure 6 (A)** Western Blot of human astrocytoma WHO grade I - IV and normal brain tissue for the expression of eIF3a, 3b, 3c, 3d, 3i, phospho-eIF4b, eIF4b and 4e. GAPDH used as a loading control. **(B-J)** Box plots for the density analysis of the Western Blots. Relative density describes the fold change of densities of tumor samples compared to normal brain tissue.

**Table 1** Density analysis of the Western Blots for eIF3a, 3q (H-300), 3b, 3c, 3d, 3i, phospho-eIF4b, eIF4b and 4e.

**Area**

|  | eIF3a | eIF3q(H-300) | eIF3b | eIF3c | eIF3d | eIF3i | phospho-eIF4b | eIF4b | eIF4e |
|---|---|---|---|---|---|---|---|---|---|
| NT | 97.536 | 258.678 | 1224.134 | 746.749 | 4440.832 | 3295.690 | 16.121 | 18.536 | 8106.702 |
| NT | 2932.175 | 118.950 | 1024.820 | 1431.134 | 5881.693 | 3133.447 | 8.121 | 1857.790 | 14065.350 |
| I | 642.021 | 174.435 | 1050.305 | 148.778 | 3994.933 | 2606.719 | 30.121 | 113.071 | 6083.388 |
| I | 23695.271 | 5209.317 | 4241.953 | 11480.116 | 16620.907 | 8187.116 | 2904.790 | 51.950 | 7269.388 |
| I | 18293.836 | 7638.660 | 5474.560 | 7074.267 | 5132.004 | 9157.087 | 2849.497 | 42.364 | 14623.765 |
| II | 21698.442 | 3639.882 | 3692.368 | 8347.045 | 10560.927 | 7314.359 | 6799.874 | 141.071 | 18873.442 |
| II | 25846.049 | 4994.974 | 7491.388 | 6251.681 | 10947.208 | 9656.794 | 8748.945 | 30.950 | 32948.283 |
| II | 23315.927 | 3338.225 | 9959.894 | 36769.798 | 13933.714 | 10863.865 | 10027.865 | 698.678 | 42550.910 |
| III | 19509.806 | 4023.246 | 3882.338 | 6532.510 | 12717.078 | 5402.267 | 13053.329 | 289.263 | 38830.889 |
| III | 19618.271 | 3821.317 | 3615.610 | 12532.894 | 6530.191 | 7467.894 | 13461.744 | 5086.075 | 43278.324 |
| III | 27356.149 | 2633.782 | 2065.711 | 19409.936 | 18153.697 | 17596.714 | 22276.735 | 11826.187 | 31652.697 |
| IV | 2249.062 | 2601.276 | 426.042 | 14.121 | 3177.305 | 3552.690 | 3032.104 | 59.243 | 10394.844 |
| IV | 11869.258 | 1339.527 | 3034.246 | 4710.024 | 8001.309 | 6680.945 | 8831.894 | 595.042 | 7045.581 |
| IV | 9312.773 | 5375.167 | 511.042 | 642.678 | 14499.986 | 5649.681 | 4142.225 | 455.092 | 20577.605 |

**Relative density**

|  | eIF3a | eIF3q(H-300) | eIF3b | eIF3c | eIF3d | eIF3i | phospho-eIF4b | eIF4b | eIF4e |
|---|---|---|---|---|---|---|---|---|---|
| NT | 1 | 1 | 1 | 1 | 1 | 1 | 1 | 1 | 1 |
| I | 0.219 | 1.466 | 1.025 | 0.104 | 0.679 | 0.832 | 3.709 | 0.061 | 0.433 |
| I | 8.081 | 43.794 | 4.139 | 8.022 | 2.826 | 2.613 | 357.689 | 0.028 | 0.517 |
| I | 6.239 | 64.217 | 5.342 | 4.943 | 0.873 | 2.922 | 350.880 | 0.023 | 1.040 |
| II | 7.400 | 30.600 | 3.603 | 5.832 | 1.796 | 2.334 | 837.320 | 0.076 | 1.342 |
| II | 8.815 | 41.992 | 7.310 | 4.368 | 1.861 | 3.082 | 1077.324 | 0.017 | 2.343 |
| II | 7.952 | 28.064 | 9.719 | 25.693 | 2.369 | 3.467 | 1234.807 | 0.376 | 3.025 |
| III | 6.654 | 33.823 | 3.788 | 4.565 | 2.162 | 1.724 | 1607.355 | 0.156 | 2.761 |
| III | 6.691 | 32.125 | 3.528 | 8.757 | 1.110 | 2.383 | 1657.646 | 2.738 | 3.077 |
| III | 9.330 | 22.142 | 2.016 | 13.563 | 3.086 | 5.616 | 2743.102 | 6.366 | 2.250 |
| IV | 0.767 | 21.869 | 0.416 | 0.010 | 0.540 | 1.134 | 373.366 | 0.032 | 0.739 |
| IV | 4.048 | 11.261 | 2.961 | 3.291 | 1.360 | 2.132 | 1087.538 | 0.320 | 0.501 |
| IV | 3.176 | 45.188 | 0.499 | 0.449 | 2.465 | 1.803 | 510.063 | 0.245 | 1.463 |
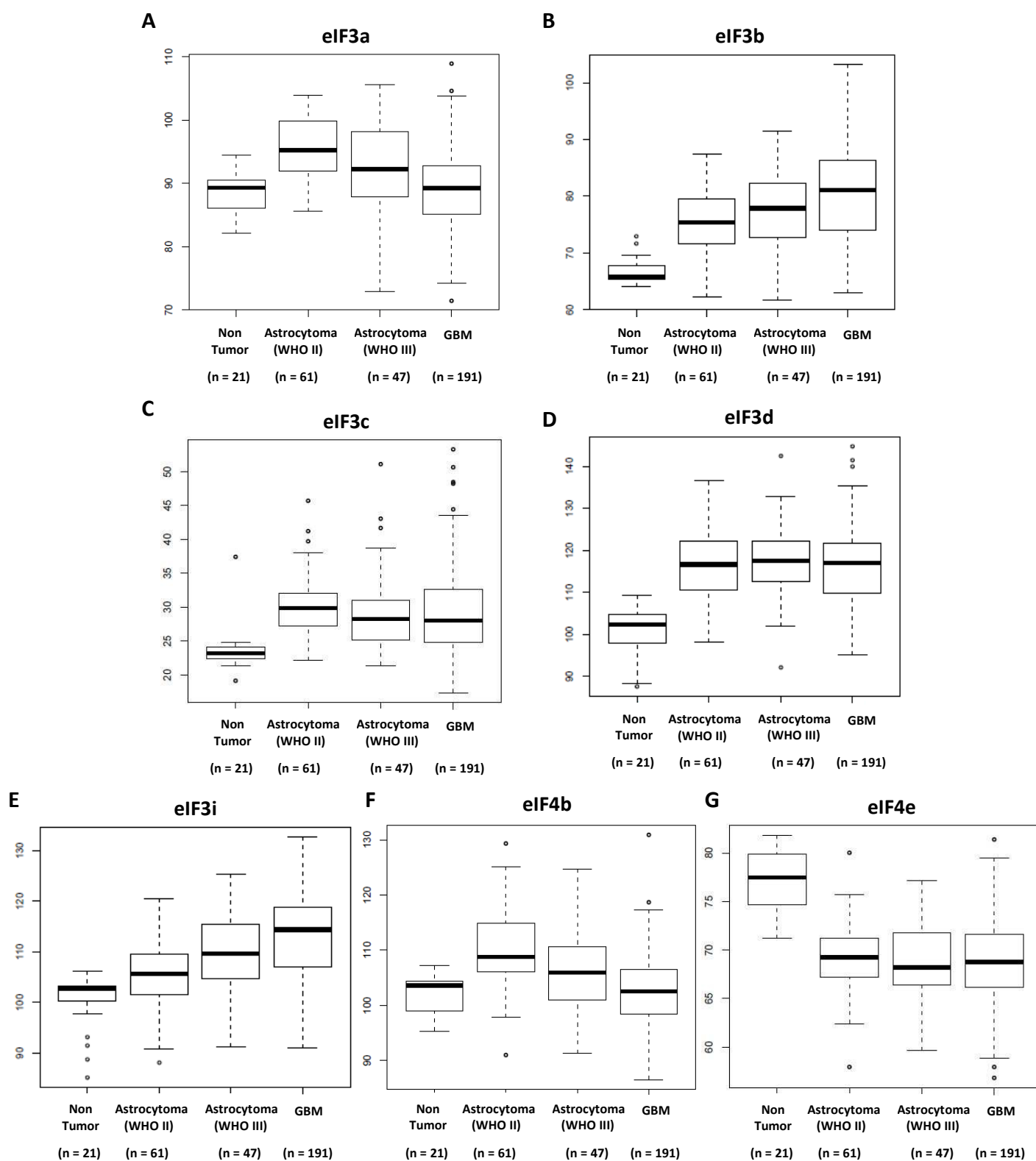
**Figure 7 (A-G)** Box plots of the REMBRANDT data of eIF3a, 3c, 4b and 4e for 21 non tumors, 61 WHO grade II, 47 grade III and 191 grade IV gliomas (GBM).
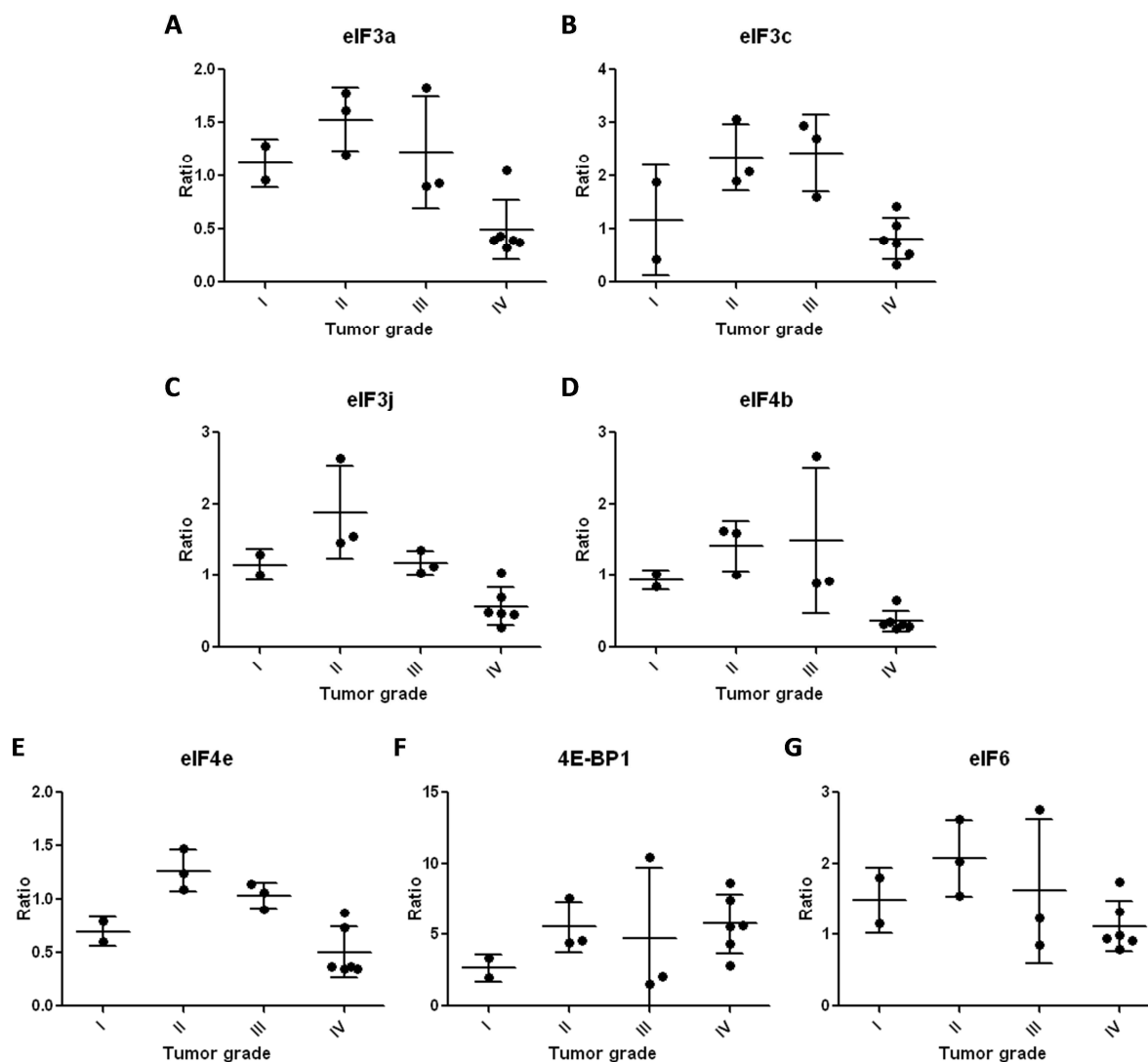
**Figure 8 (A-G) Real-time RT-PCR of eIFs in human astrocytoma WHO grade I- IV and normal brain tissue.** Relative quantification of eIF3a, eIF3c, eIF3j, eIF4b, eIF4e, 4E-BP1 and eIF6 was performed with real-time RT-PCR**.** The ration describes the mRNA expression changes of the target genes in tumor tissue compared to normal brain.

### 5.1.2 Immunostaining of eIFs in human glioma tissue

The expression of eIF3a, eIF3c and eIF4e in the immunostained samples was evaluated by two independent observers (C. Ernst, J. Haybaeck). The localization of eIF3a was predominantly cytoplasmic, as well as endothelial in some cases (Figure 9). In GBMs a tendency for a higher staining intensity of tumor cells was observed compared to low grade and anaplastic astrocytomas. The analyzed grade IV tumors were all stained positive for eIF3a, with predominantly weak and strong TIS (40% and 47%, respectively). This indicates an elevated expression of eIF3a in these gliomas. In contrast, only 53% of the grade I astrocytomas were positive for eIF3a.

Statistical analysis revealed a significant difference in the intensity of eIF3a expression in tumor cells between astroytomas of grade I and IV (Mann Whitney U Test, $p$ = 0.031), as well as III and IV ($p$ = 0.022). For endothelial staining, significant differences for grade I and IV ($p$ = 0.042), II and IV ($p$ < 0.001), and between III and IV ($p$ < 0.0001) could be observed.

The staining of tumor cells for eIF3c was generally strong, with predominant cytoplasmic localization (Figure 10). Of the analyzed grade III astroytomas 35% had a strong TIS for eIF3c, as compared to grade I and IV astroytomas with 79% and 60%, respectively. No statistical differences of eIF3c staining between the tumor grades were observed.

For eIF4e the immunostaining was comparatively weak (Figure 11). 43% of the analyzed glioma samples were negative for eIF4e. No significant differences between the tumor grades were detected. Endothelial staining for eIF3c and eIF4e was highly heterogeneous and ambiguous and therefore was not evaluated.

Comparison of lower (WHO grade I and II) and higher grade (III and IV) revealed no statistically significant differences in expression of any of the evaluated eIF subunits.
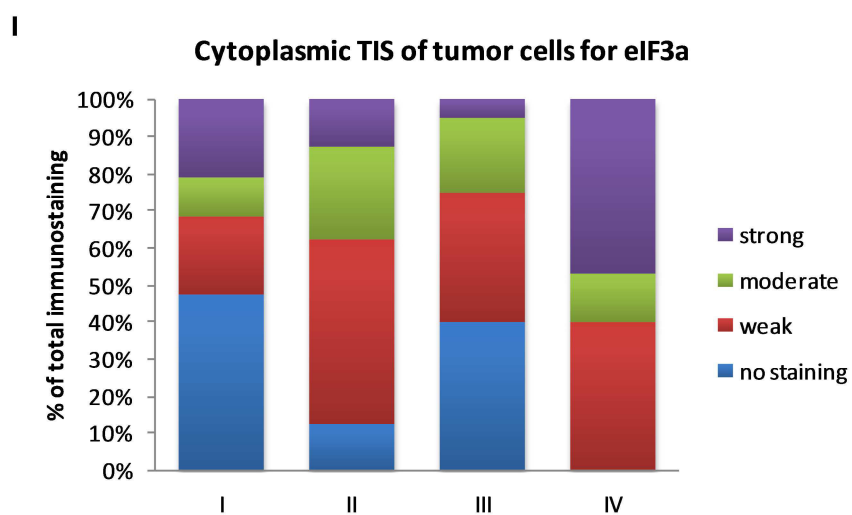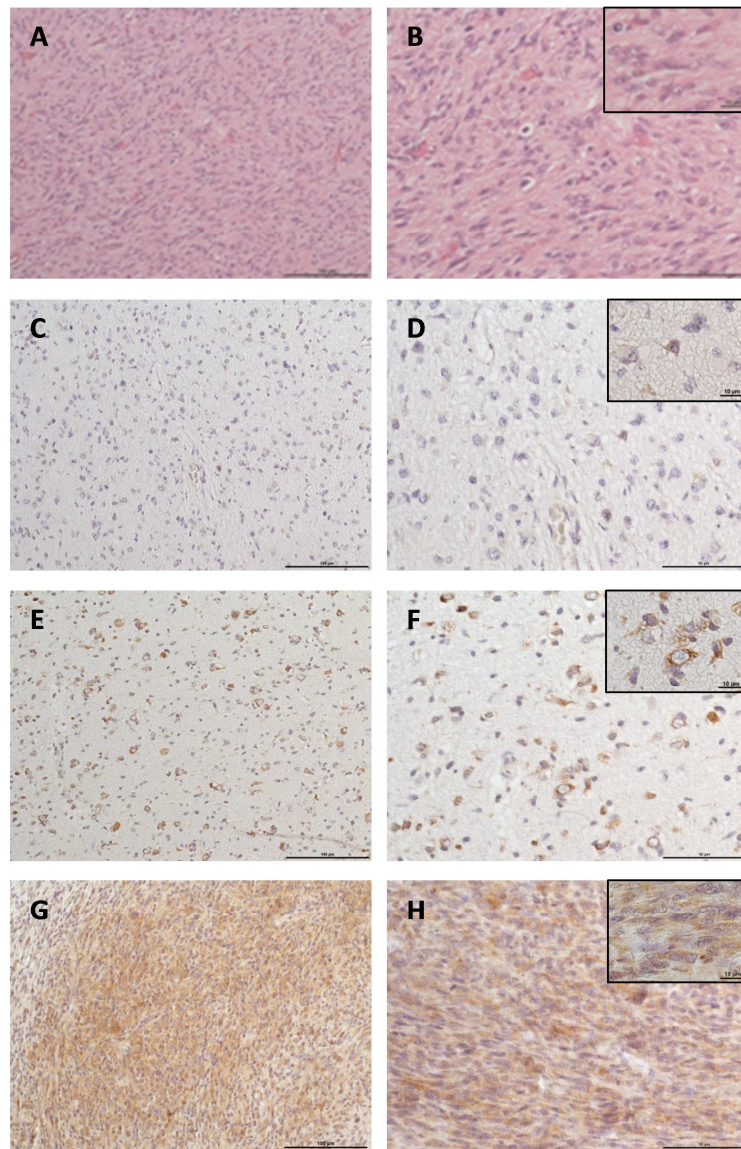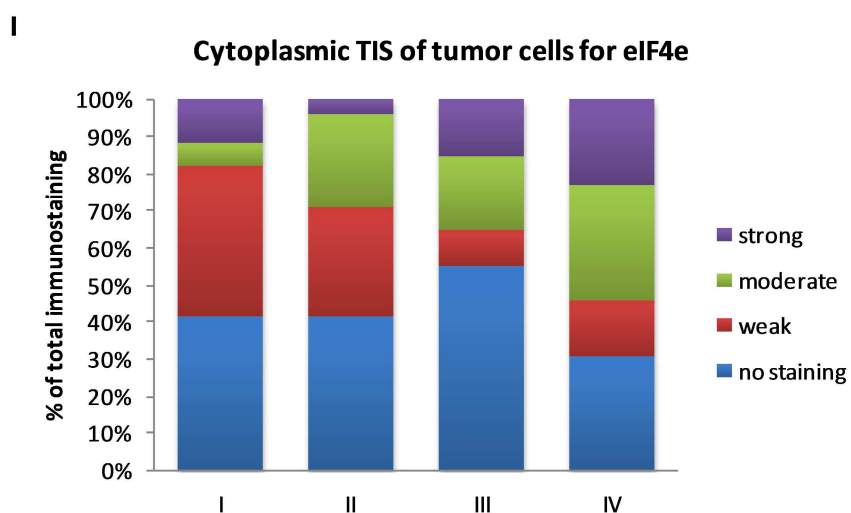
**Figure 9 Immunostaining of astrocytoma sections for eIF3a. (A, B)** HE stainings of astrocytomas (B inset, higher magnification). **(C-H)** Astrocytoma sections positive for eIF3a. Examples for weak (C, D, inset with higher magnification), moderate (E, F, inset with higher magnification) and strong reactivity (G, H, inset with higher magnification). Scale bars, 100 μm (A, C, E, G), 50 μm (B, D, F, H) and 10 μm (B, D, F, H insets). **(I)** Total immunostaining score (TIS) of tumor cells of astrocytomas WHO grade I, II, III and IV for cytoplasmic eIF3a.
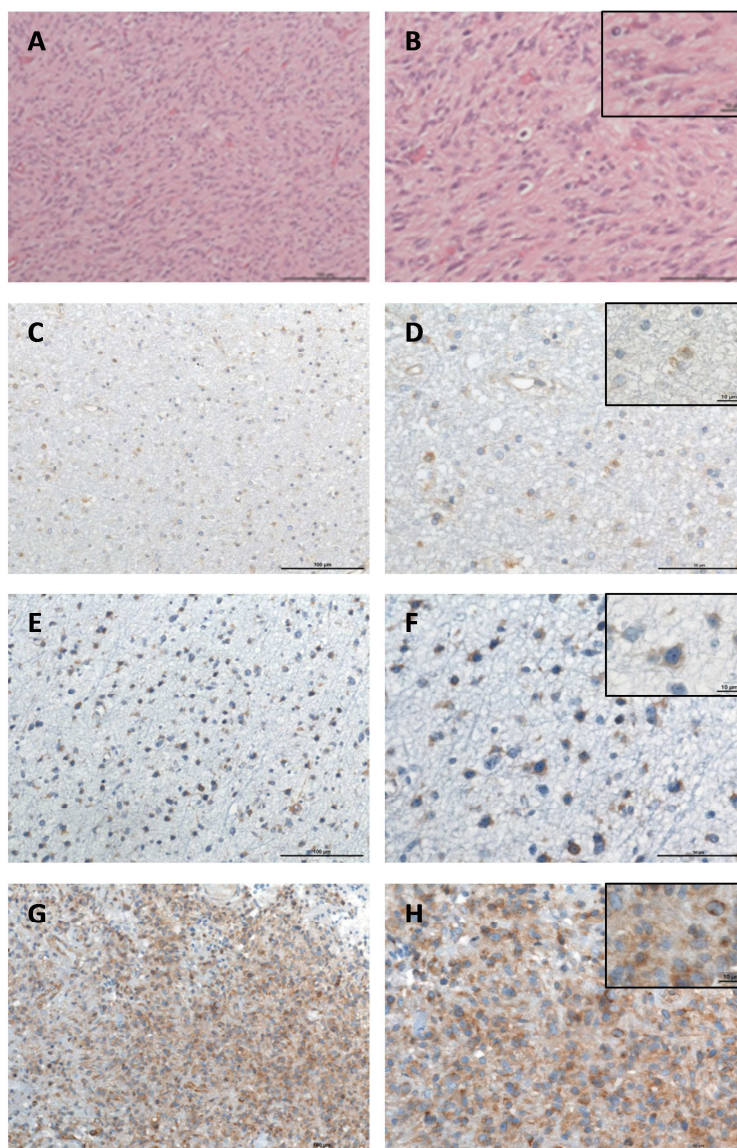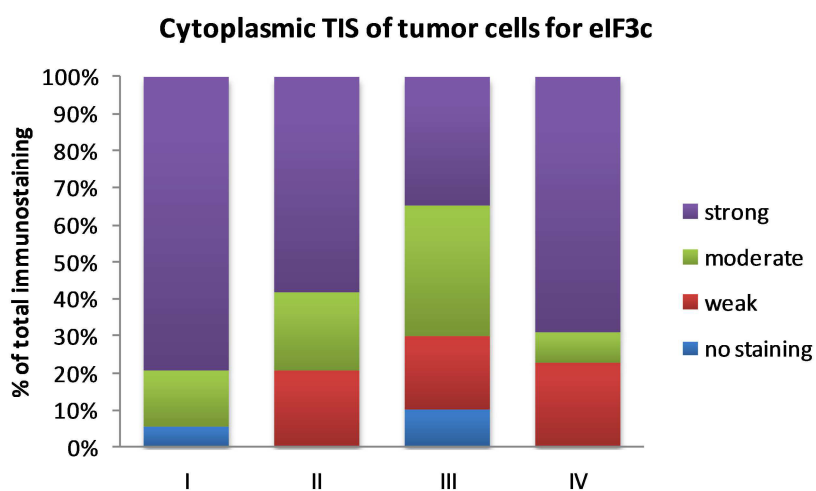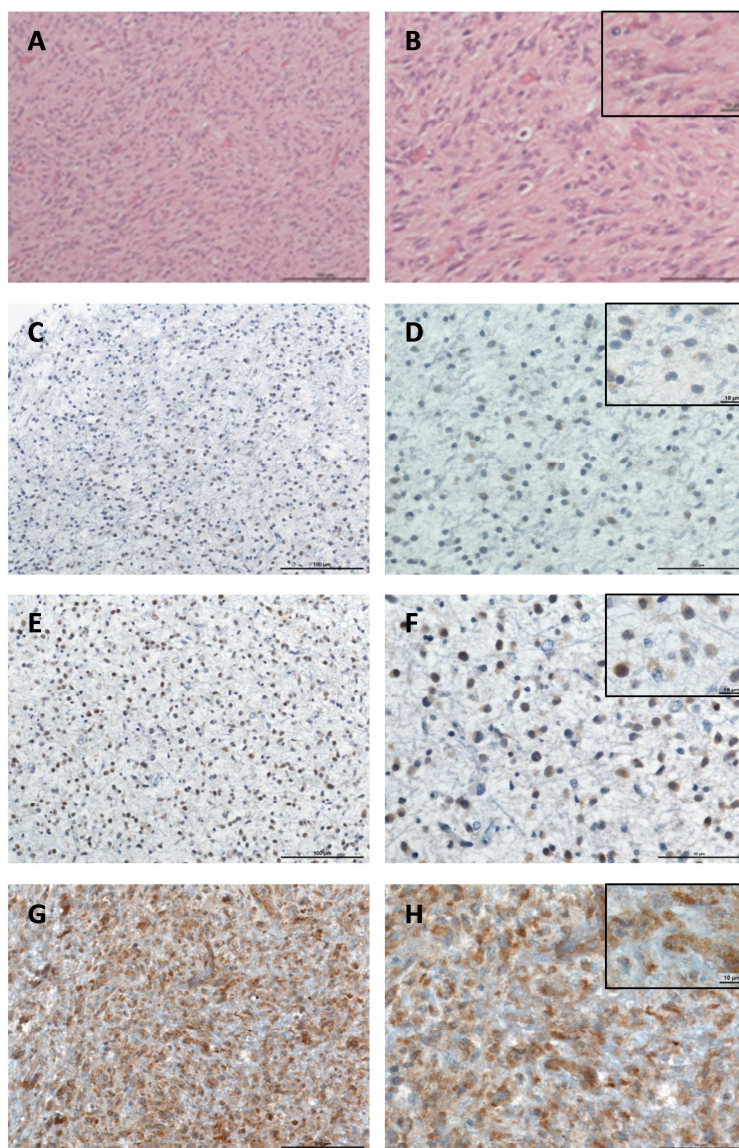
**Figure 10 Immunostaining of astrocytoma sections for eIF3c. (A, B)** HE stainings of astrocytomas (B inset, higher magnification). **(C-H)** Astrocytoma sections positive for eIF3c. Examples for weak (C, D, inset with higher magnification), moderate (E, F, inset with higher magnification) and strong reactivity (G, H, inset with higher magnification). Scale bars, 100 μm (A, C, E, G), 50 μm (B, D, F, H) and 10 μm (B, D, F, H insets). **(I)** Total immunostaining score (TIS) of tumor cells of astrocytomas WHO grade I, II, III and IV for cytoplasmic eIF3c.

**Figure 11 Immunostaining of astrocytoma sections for eIF4e. (A, B)** HE stainings of astrocytomas (B inset, higher magnification). **(C-H)** Astrocytoma sections positive for eIF4e. Examples for weak (C, D, inset with higher magnification), moderate (E, F, inset with higher magnification) and strong reactivity (G, H, inset with higher magnification). Scale bars, 100 µm (A, C, E, G), 50 µm (B, D, F, H) and 10 µm (B, D, F, H insets). **(I)** Total immunostaining score (TIS) of tumor cells of astrocytomas WHO grade I, II, III and IV for cytoplasmic eIF4e.

28

## 5.2 mTOR signaling in human glioma tissue

The role of the RTK/PI3K/Akt/mTOR pathway in the glioma samples was investigated with Western Blot analysis. As shown in Figure 13A, the analyzed members of this pathway showed a broad spectrum of expression within and between the different astrocytoma grades. Protein levels of phospho-Akt, phospho-p70S6K, phospho-4E-BP1 and 4E-BP1 were highest in GBMs, as compared to normal brain tissue and low grade and anaplastic astrocytomas (grade I − III) (Figure 13B-I, Table 2). The relative density of phospho-Akt, phospho-p70S6K and phospho-4E-BP1, analyzed with the ImageJ software, was 500 − 800 times increased. The expression of PTEN and mTOR was decreased in GBMs, whereas Akt and p70S6K expression remained comparatively constant throughout the tested samples (Figure 13B-I).

According to the REMBRANDT data analysis no significant changes in gene expression were observed for Akt, PTEN, mTOR and p70S6K (Figure 12). The box plot for 4E-BP1 showed an increased mRNA level within the tumors, which was reproduced by Western blotting.
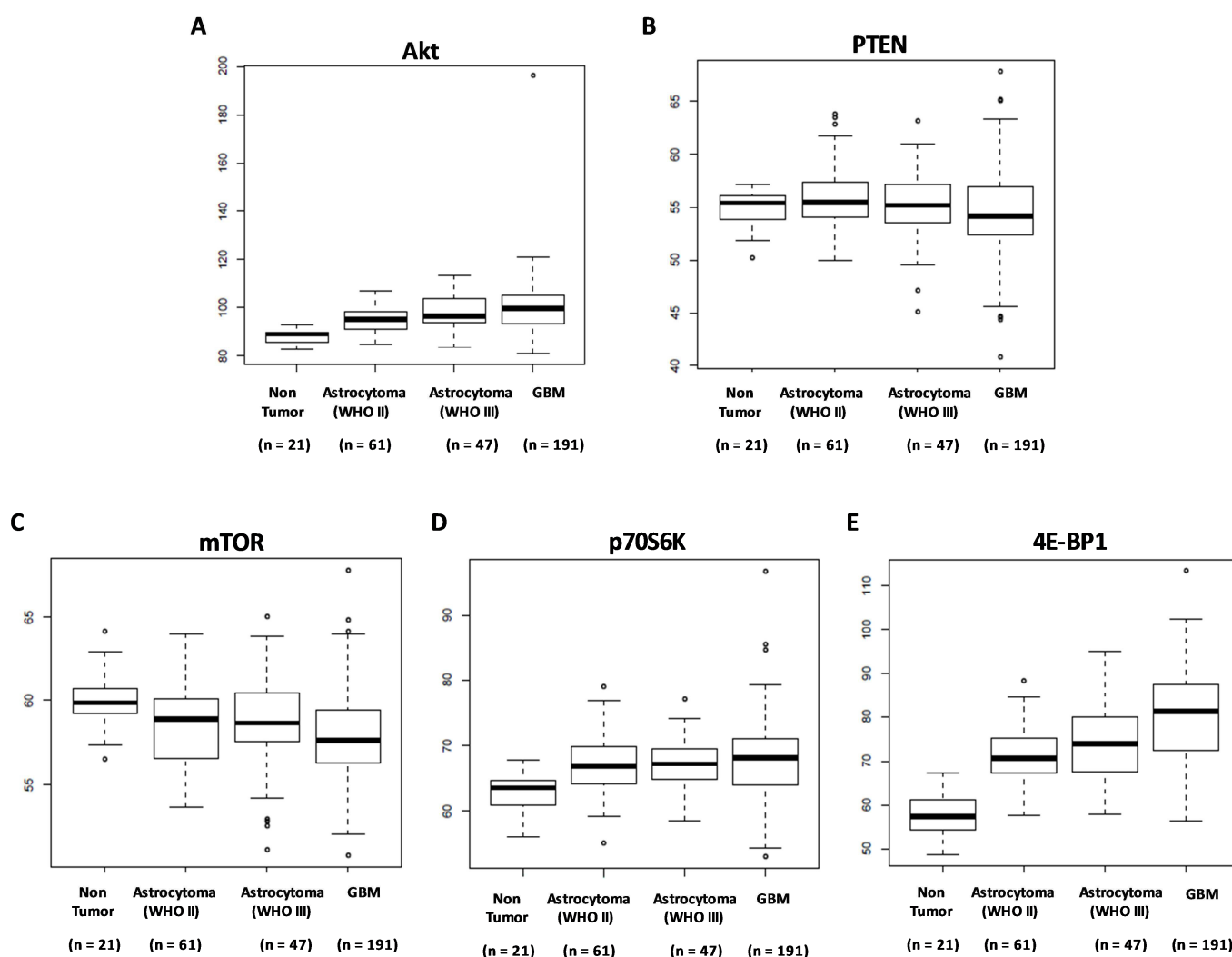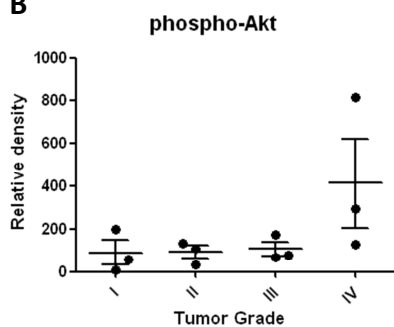


**Figure 12 (A-E)** Box plots of the REMBRANDT data of Akt, PTEN, mTOR, p70S6K and 4E-BP1 for 21 non tumors, 61 WHO grade II, 47 grade III and 191 grade IV gliomas (GBM).
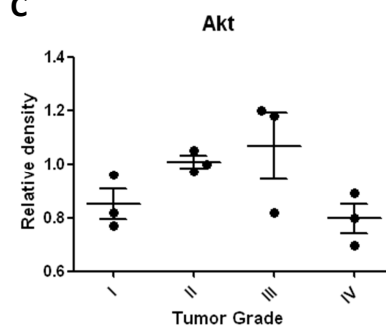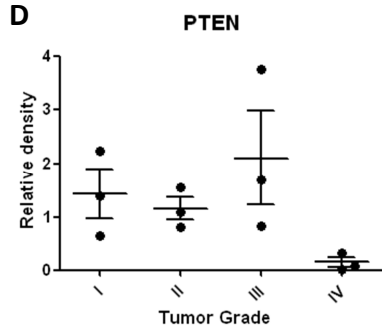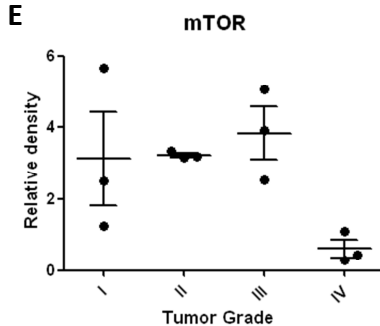
**A**
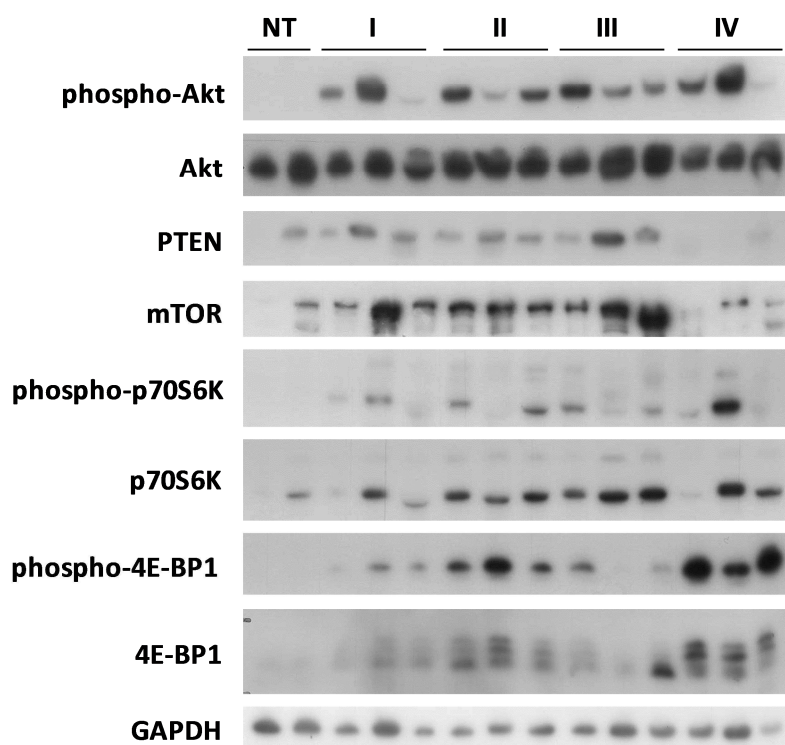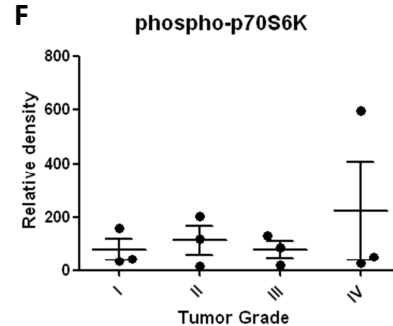


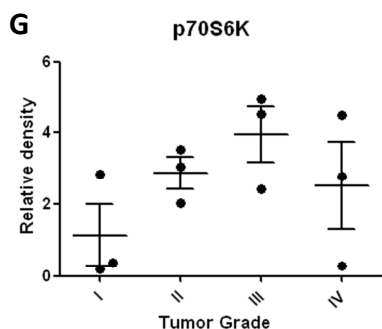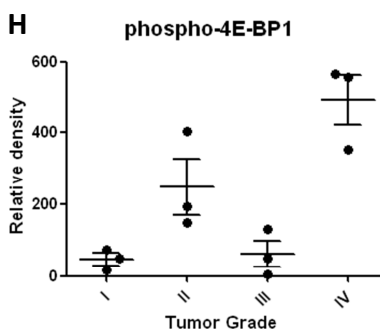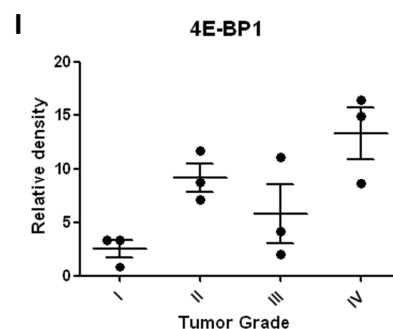**Figure 13 (A)** Western Blot of human astrocytoma WHO Grade I - IV and normal brain tissue for the expression of phospho-Akt, Akt, PTEN, mTOR, phospho-p70S6K, p70S6K, phospho-4E-BP1 and 4E-BP1. GAPDH used as a loading control. **(B-I)** Box plots for the density analysis of the Western Blots. Relative density describes the fold change of densities of tumor samples compared to normal brain tissue.

**Table 2** Density analysis of the Western Blots for phospho-Akt, Akt, PTEN, mTOR, phospho-p70S6K (p-p70S6K), p70S6K, phospho-4E-BP1 (p-4E-BP1) and 4E-BP1.

**Area**

|  | phospho-Akt | Akt | PTEN | mTOR | p-p70S6K | p70S6K | p-4E-BP1 | 4E-BP1 |
|---|---|---|---|---|---|---|---|---|
| NT | 50.121 | 24058.948 | 176.364 | 38.536 | 34.121 | 78.364 | 22.121 | 1865.648 |
| NT | 121.536 | 34579.676 | 5181.853 | 3393.125 | 30.121 | 3532.296 | 75.536 | 3190.719 |
| I | 7021.116 | 26673.948 | 3437.933 | 4204.196 | 1263.234 | 710.335 | 1176.749 | 2867.962 |
| I | 24268.806 | 33127.605 | 11606.258 | 19175.777 | 4750.853 | 10027.530 | 5611.924 | 10833.794 |
| I | 1033.406 | 28370.070 | 7182.874 | 8505.894 | 1069.263 | 1363.447 | 3745.104 | 10874.702 |
| II | 16465.279 | 33588.484 | 4239.418 | 11379.258 | 3614.903 | 10734.338 | 14552.371 | 27779.756 |
| II | 4069.125 | 36239.919 | 8086.530 | 10892.844 | 498.435 | 7178.338 | 30525.040 | 37071.019 |
| II | 12976.380 | 34499.383 | 5678.095 | 10705.430 | 6095.631 | 12521.652 | 11251.501 | 22445.250 |
| III | 21158.836 | 28444.605 | 4344.660 | 8618.652 | 3941.660 | 8504.995 | 9925.915 | 13247.581 |
| III | 8511.116 | 40689.090 | 19465.643 | 13333.765 | 568.406 | 16010.380 | 268.849 | 6677.246 |
| III | 9280.380 | 41423.726 | 8817.652 | 17154.546 | 2613.690 | 17446.016 | 3852.619 | 35352.789 |
| IV | 15669.300 | 24107.463 | 397.778 | 1500.648 | 1529.305 | 1006.991 | 42688.203 | 52337.789 |
| IV | 35674.040 | 27686.655 | 124.657 | 3719.711 | 17867.350 | 15832.501 | 26763.555 | 47465.245 |
| IV | 98779.087 | 30829.697 | 1745.406 | 942.113 | 797.920 | 9809.116 | 42145.082 | 27414.028 |

**Relative density**

|  | phospho-Akt | Akt | PTEN | mTOR | p-p70S6K | p70S6K | p-4E-BP1 | 4E-BP1 |
|---|---|---|---|---|---|---|---|---|
| NT | 1 | 1 | 1 | 1 | 1 | 1 | 1 | 1 |
| I | 57.770 | 0.771 | 0.663 | 1.239 | 41.939 | 0.201 | 15.579 | 0.899 |
| I | 199.684 | 0.958 | 2.240 | 5.651 | 157.726 | 2.839 | 74.295 | 3.395 |
| I | 8.503 | 0.820 | 1.386 | 2.507 | 35.499 | 0.386 | 49.580 | 3.408 |
| II | 135.477 | 0.971 | 0.818 | 3.354 | 120.013 | 3.039 | 192.655 | 8.706 |
| II | 33.481 | 1.048 | 1.561 | 3.210 | 16.548 | 2.032 | 404.112 | 11.618 |
| II | 106.770 | 0.998 | 1.096 | 3.155 | 202.371 | 3.545 | 148.955 | 7.035 |
| III | 174.095 | 0.823 | 0.838 | 2.540 | 130.861 | 2.408 | 131.406 | 4.152 |
| III | 70.030 | 1.177 | 3.757 | 3.930 | 18.871 | 4.533 | 3.559 | 2.093 |
| III | 76.359 | 1.198 | 1.702 | 5.056 | 86.773 | 4.939 | 51.004 | 11.080 |
| IV | 128.927 | 0.697 | 0.077 | 0.442 | 50.772 | 0.285 | 565.137 | 16.403 |
| IV | 293.527 | 0.801 | 0.024 | 1.096 | 593.186 | 4.482 | 354.315 | 14.876 |
| IV | 812.756 | 0.892 | 0.337 | 0.278 | 26.490 | 2.777 | 557.947 | 8.592 |

## 5.3 Cell culture

A first characterization of the GBM cells was performed with Western Blot analysis using antibodies directed against eIF3c and eIF3d (Figure 14). No differences in expression of the tested proteins in the different cell lines were found. The primary cell cultures are pictured in Figure 15.

Due to time reasons I was not able to finish any further cell culture experiments during the course of my master thesis.
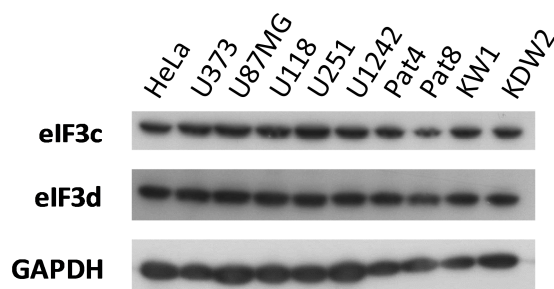


**Figure 14** Western Blot of 5 human GBM cell lines (U373, U87MG, U118, U251 and U1242), 4 primary GBM cell cultures (Pat4, Pat8, KW1 and KDW2) and HeLa cells for the expression of eIF3c and eIF3d. GAPDH used as a loading control.
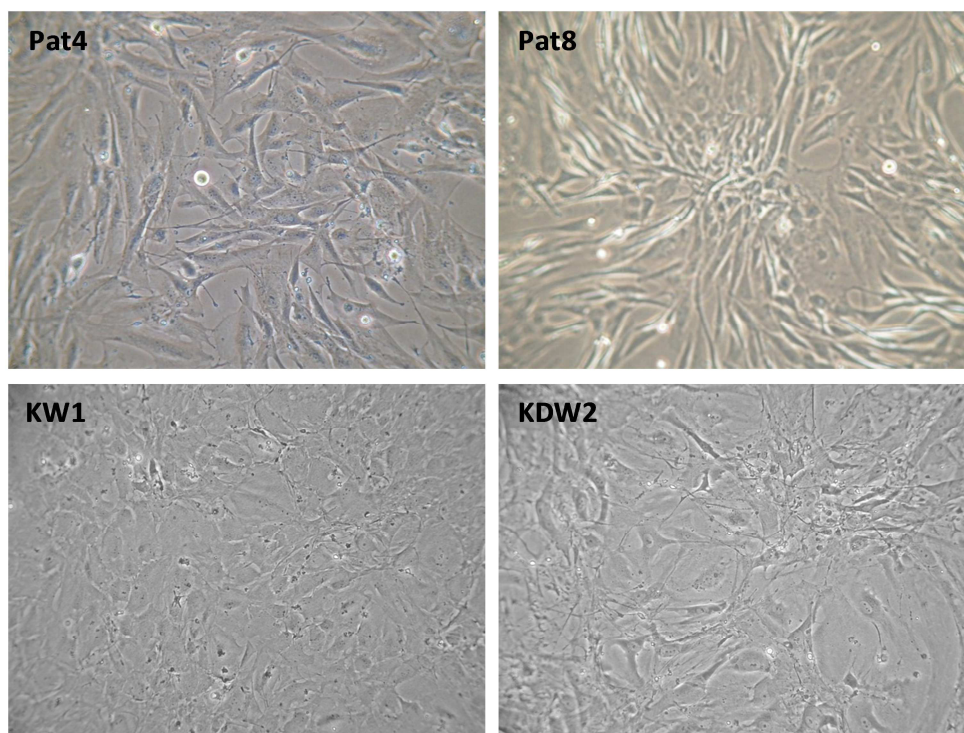


**Figure 15** Phase contrast photos of the primary GBM cells Pat4, Pat8, KW1 and KDW2 (200x magnification).

# 6   Discussion

Changes in translational control play a pivotal role in deregulation of cell proliferation and tumor formation underlying uncontrolled cell growth. Since almost all eIFs are linked to various types of cancer but have not yet been studied in glial differentiated tumors, the aim of this project was to investigate the contribution of a subset of eIFs in glioma development, mainly focusing on GBM. By performing histological and immunohistochemical stainings, Western Blot and real-time RT-PCR analysis, cell culture experiments and carefully analyzing already existing oligo microarray tumor data sets of astrocytomas of WHO grade I - IV, an expression pattern for specific eIFs could be made. This might help understanding the role of eIFs in GBM formation and glioma progression in order to design new therapies in addition to surgical resection, radiation and the so far established chemotherapy with the aim of prolonging the life span of glioma patients. In addition, we checked the expression pattern of members of the mTOR pathway.

Interestingly, we were able to show an alternating expression pattern of most of the investigated eIF subunits. The expression of eIF3a, eIF3b, eIF3c, phospho-eIF4b, eIF4b and eIF4e seems to be promoted in lower grade gliomas compared to healthy brain specimens and depleted in highest grade astrocytomas. Accordingly, increased eIF levels might be responsible for tumor formation and be associated with a less aggressive behavior, whereas loss of expression may lead to progression into the most malignant tumor grade. This is in line with previous findings, stating that over-expression of eIF3a is reversed in high malignancy stages of cervix, esophageal and gastric cancer[1–3]. On the other hand, immunohistochemical analysis showed a correlation of eIF3a expression with tumor grade, with highest levels in GBMs, but no significant changes for eIF3c and eIF4e.

Of the analyzed eIFs, solely eIF3b has already been linked to gliomas[4]. Knockdown of eIF3b with a specific shRNA construct has been shown to inhibit proliferation and promote apoptosis in human U87MG GBM cells. This illustrates the importance of similar experimental setups using knockdown-constructs to manipulate eIF expression in human glioma cell lines to discover those subunits crucial for gliomagenesis.

Above all, what needs to be considered in our study is the heterogeneity of eIF levels among different tumor specimens of the same entity. One of the three astrocytoma grade I samples we subjected to Western Blot analysis had a completely distinct expression profile of all of

the tested eIFs than the other two tumors. Also the three GBM samples differ in their expression of some of the analyzed proteins. Expression of eIF3a and eIF3d, for instance, is decreased in one sample and increased in the other two GBM specimens. This leads to the assumption, that these translational regulatory proteins are expressed quite heterogenously among different tumor specimens of the same entity. Therefore we suggest to analyze a larger cohort of glioma samples. Likewise, the number of samples subjected to rel-time RT-PCR is too small regarding lower grade and anaplastic astrocytomas (grade I – III). For tumors of WHO grade I only two specimens were analyzed, which does not allow a statistically significant evaluation. To reduce standard deviation, the sample number needs to be increased.

Constitutive activation of mTOR signaling is a hallmark of GBM[5]. The mammalian target of rapamycin (mTOR) regulates both cell growth and cell cycle progression. It has been proposed to promote survival and astrocytic characteristics in GBM and might be involved in glioma formation[6,7]. Blockade of mTOR in a mouse GBM model resulted in conversion of GBM cells to an oligodendroglioma-like morphology in the treated tumors[8]. mTOR is a downstream target of Akt, which is activated in approximately 70% of GBMs[8]. Akt activation is associated with loss of function of the tumor suppressor PTEN, which is the case in about 50% of human GBMs. PTEN is the major negative regulator in this signaling pathway[9]. mTOR further downstream phosphorylates p70S6K and 4E-BP1, two key regulators of protein synthesis. In our study we found elevated levels of phospho-Akt, phospho-p70S6K, phospho-4E-BP1 and 4E-BP1 in GBMs compared to normal brain and lower grade tumors, while the inactive, unphosphorylated forms of Akt and p70S6K did not show significant alterations, which is in accordance with the literature[9]. As for PTEN, expression is completely lost in the tested GBM samples. This fits with previous findings, stating that ~50% of GBMs have *PTEN* deletion, mutation or loss of function[8]. Since we found mTOR levels to be reduced in GBM relative to lower grade tumors it would also be important to check levels of the activated protein. In a previous study phospho-mTOR was shown to increase with histological grade of astrocytic and oligodendrocytic tumors and inhibition of mTOR with rapamycin reduced proliferation of GBM cells *in vitro*[10,11].

Upon phosphorylation of 4E-BP1 the translation initiation factor eIF4e is released from the complex with its binding protein and can enhance cap-dependent translation through

interaction with the eIF4F complex[12]. Our protein analysis revealed distinctly increased levels of phospho-4E-BP1, which might indicate promotion of cap-dependant translation initiation through the activation of eIF4e. The rather slight changes in eIF4e levels in normal brain and tumor tissue can be explained as by the detergent conditions during SDS-PAGE protein complexes get disintegrated. Thus, Western Blotting only pictures the total amount of eIF4e and does not distinguish between the active and inactive form.

This project was a preliminary trial to characterize the expression of eIFs in relation to the mTOR signaling pathway in human astrocytomas and to assess their possible use for targeted therapy. In order to achieve this, further experiments will be needed. First, additional cell culture experiments will be important to first completely characterize human GBM cell lines and primary tumor cells and in a next step to treat them with specific knock down constructs as well as with mTOR inhibitors and today's commonly used chemotherapeutics. Those *in vitro* experiments could then be transferred into *in vivo* models with mice or rats and offer a basis for the development of new drugs for GBM patients. Most eligible treatment strategies to fight this aggressive cancer entity might be a combination of eIF and/or mTOR inhibitors with chemo-radiotherapy. Given that gliomas evolve through a multi-step process and are very heterogeneous tumors, as confirmed by this study, several treatment strategies specific for each patient will need to be combined[13].

# 7    References

1.      Kleihues, P. *et al.* The WHO classification of tumors of the nervous system. *J. Neuropathol. Exp. Neurol.* **61**, 215–225; discussion 226–229 (2002).

2.      Zhang, X., Zhang, W., Cao, W.-D., Cheng, G. & Zhang, Y.-Q. Glioblastoma multiforme: Molecular characterization and current treatment strategy (Review). *Exp Ther Med* **3**, 9–14 (2012).

3.      Kleihues, P., Soylemezoglu, F., Schäuble, B., Scheithauer, B. W. & Burger, P. C. Histopathology, classification, and grading of gliomas. *Glia* **15**, 211–221 (1995).

4.      Van Meir, E. G. *et al.* Exciting new advances in neuro-oncology: the avenue to a cure for malignant glioma. *CA Cancer J Clin* **60**, 166–193 (2010).

5.      Louis, D. N., Ohgaki, H., Wiestler, O. D. & Cavenee, W. K. *WHO Classification of Tumours of the Central Nervous System*. (IARC, 2007).

6.      Ng, K., Kim, R., Kesari, S., Carter, B. & Chen, C. C. Genomic profiling of glioblastoma: convergence of fundamental biologic tenets and novel insights. *J. Neurooncol.* **107**, 1–12 (2012).

7.      Kleihues, P. & Ohgaki, H. Primary and secondary glioblastomas: from concept to clinical diagnosis. *Neuro-oncology* **1**, 44–51 (1999).

8.      Ohgaki, H. *et al.* Genetic pathways to glioblastoma: a population-based study. *Cancer Res.* **64**, 6892–6899 (2004).

9.      Ohgaki, H. & Kleihues, P. Genetic pathways to primary and secondary glioblastoma. *Am. J. Pathol.* **170**, 1445–1453 (2007).

10.     The Cancer Genome Atlas (TCGA) Research Network Comprehensive genomic characterization defines human glioblastoma genes and core pathways. *Nature* **455**, 1061–1068 (2008).

11.     Verhaak, R. G. W. *et al.* Integrated genomic analysis identifies clinically relevant subtypes of glioblastoma characterized by abnormalities in PDGFRA, IDH1, EGFR, and NF1. *Cancer Cell* **17**, 98–110 (2010).

12.     Hutterer, M., Gunsilius, E. & Stockhammer, G. Molecular therapies for malignant glioma. *Wien Med Wochenschr* **156**, 351–363 (2006).

13.     Clarke, J., Butowski, N. & Chang, S. Recent advances in therapy for glioblastoma. *Arch. Neurol.* **67**, 279–283 (2010).

14.     Ohka, F., Natsume, A. & Wakabayashi, T. Current trends in targeted therapies for glioblastoma multiforme. *Neurol Res Int* **2012**, 878425 (2012).

15.     Van den Bent, M. J. *et al.* Randomized phase II trial of erlotinib versus temozolomide or carmustine in recurrent glioblastoma: EORTC brain tumor group study 26034. *J. Clin. Oncol.* **27**, 1268–1274 (2009).

16.     Fan, Q.-W. & Weiss, W. A. Targeting the RTK-PI3K-mTOR axis in malignant glioma: overcoming resistance. *Curr. Top. Microbiol. Immunol.* **347**, 279–296 (2010).

17.     Akhavan, D., Cloughesy, T. F. & Mischel, P. S. mTOR signaling in glioblastoma: lessons learned from bench to bedside. *Neuro-oncology* **12**, 882–889 (2010).

18.     Hegi, M. E. *et al.* MGMT gene silencing and benefit from temozolomide in glioblastoma. *N. Engl. J. Med.* **352**, 997–1003 (2005).

19.     Eramo, A. *et al.* Chemotherapy resistance of glioblastoma stem cells. *Cell Death Differ.* **13**, 1238–1241 (2006).

20.     Sonenberg, N. & Hinnebusch, A. G. Regulation of translation initiation in eukaryotes: mechanisms and biological targets. *Cell* **136**, 731–745 (2009).

21.     Silvera, D., Formenti, S. C. & Schneider, R. J. Translational control in cancer. *Nat. Rev. Cancer* **10**, 254–266 (2010).

22.     Gingras, A.-C., Raught, B. & Sonenberg, N. eIF4 INITIATION FACTORS: Effectors of mRNA Recruitment to Ribosomes and Regulators of Translation. *Annual Review of Biochemistry* **68**, 913–963 (1999).

23.     Pestova, T. & Kolupaeva, V. The roles of individual eukaryotic translation initiation factors in ribosomal scanning and initiation codon selection. *Genes Dev.* **16**, 2906–2922 (2002).

24.     Kapp, L. D. & Lorsch, J. R. The molecular mechanics of eukaryotic translation. *Annu. Rev. Biochem.* **73**, 657–704 (2004).

25.     Watkins, S. J. & Norbury, C. J. Translation initiation and its deregulation during tumorigenesis. *Br. J. Cancer* **86**, 1023–1027 (2002).

26.     Bachmann, F., Bänziger, R. & Burger, M. M. Cloning of a novel protein overexpressed in human mammary carcinoma. *Cancer Res.* **57**, 988–994 (1997).

27.     Dellas, A. *et al.* Expression of p150 in cervical neoplasia and its potential value in predicting survival. *Cancer* **83**, 1376–1383 (1998).

28.     Haybaeck, J. *et al.* Overexpression of p150, a part of the large subunit of the eukaryotic translation initiation factor 3, in colon cancer. *Anticancer Res.* **30**, 1047–1055 (2010).

29.     Pincheira, R., Chen, Q. & Zhang, J. T. Identification of a 170-kDa protein over-expressed in lung cancers. *Br. J. Cancer* **84**, 1520–1527 (2001).

30.     Chen, G. & Burger, M. M. p150 expression and its prognostic value in squamous-cell carcinoma of the esophagus. *Int. J. Cancer* **84**, 95–100 (1999).

31.     Chen, G. & Burger, M. M. p150 overexpression in gastric carcinoma: the association with p53, apoptosis and cell proliferation. *Int. J. Cancer* **112**, 393–398 (2004).

32.     Yin, J.-Y., Dong, Z., Liu, Z.-Q. & Zhang, J.-T. Translational control gone awry: a new mechanism of tumorigenesis and novel targets of cancer treatments. *Biosci. Rep.* **31**, 1–15 (2011).

33.     Liang, H. *et al.* Knockdown of eukaryotic translation initiation factors 3B (EIF3B) inhibits proliferation and promotes apoptosis in glioblastoma cells. *Neurol. Sci.* **33**, 1057–1062 (2012).

34.     Li, B. D., McDonald, J. C., Nassar, R. & De Benedetti, A. Clinical outcome in stage I to III breast carcinoma and eIF4E overexpression. *Ann. Surg.* **227**, 756–756l; discussion 761–763 (1998).

35.     Rosenwald, I. B. *et al.* Upregulation of protein synthesis initiation factor eIF-4E is an early event during colon carcinogenesis. *Oncogene* **18**, 2507–2517 (1999).

36.     Noske, A. *et al.* Activation of mTOR in a subgroup of ovarian carcinomas: correlation with p-eIF-4E and prognosis. *Oncol. Rep.* **20**, 1409–1417 (2008).

37.     Wang, R. *et al.* Overexpression of eukaryotic initiation factor 4E (eIF4E) and its clinical significance in lung adenocarcinoma. *Lung Cancer* **66**, 237–244 (2009).

38.     Gu, X., Jones, L., Lowery-Norberg, M. & Fowler, M. Expression of eukaryotic initiation factor 4E in astrocytic tumors. *Appl. Immunohistochem. Mol. Morphol.* **13**, 178–183 (2005).

39.     Mamane, Y., Petroulakis, E., LeBacquer, O. & Sonenberg, N. mTOR, translation initiation and cancer. *Oncogene* **25**, 6416–6422 (2006).

40.     Wang, S. I. *et al.* Somatic mutations of PTEN in glioblastoma multiforme. *Cancer Res.* **57**, 4183–4186 (1997).

41.     Forgacs, E. *et al.* Mutation analysis of the PTEN/MMAC1 gene in lung cancer. *Oncogene* **17**, 1557–1565 (1998).

42.    Sun, M. *et al.* AKT1/PKBalpha kinase is frequently elevated in human cancers and its constitutive activation is required for oncogenic transformation in NIH3T3 cells. *Am. J. Pathol.* **159**, 431–437 (2001).

43.    Yokoyama, Y. *et al.* Expression of PTEN and PTEN pseudogene in endometrial carcinoma. *Int. J. Mol. Med.* **6**, 47–50 (2000).

44.    Ruggero, D. Translational Control in Cancer Etiology. *Cold Spring Harbor perspectives in biology* (2012).doi:10.1101/cshperspect.a012336

45.    Jia, Y. *et al.* Design, synthesis and evaluation of analogs of initiation factor 4E (eIF4E) cap-binding antagonist Bn7-GMP. *Eur J Med Chem* **45**, 1304–1313 (2010).

46.    Borden, K. L. Targeting the oncogene eIF4E in cancer: From the bench to clinical trials. *Clin Invest Med* **34**, E315 (2011).

47.    Graff, J. R. *et al.* Therapeutic suppression of translation initiation factor eIF4E expression reduces tumor growth without toxicity. *J. Clin. Invest.* **117**, 2638–2648 (2007).

48.    National Cancer Institute Rembrandt: Home. (2005).at <http://caintegrator-info.nci.nih.gov/rembrandt>

49.    R Development Core Team *R: A language and environment for statistical computing.* (Foundation for Statistical Computing, 2011).at <http://www.r-project.org/>

50.    Gautier, L., Cope, L., Bolstad, B. M. & Irizarry, R. A. affy—analysis of Affymetrix GeneChip data at the probe level. *Bioinformatics* **20**, 307–315 (2004).

51.    Gentleman, R. annotate: Annotation for microarrays.

52.    Smyth, G.in *Bioinformatics and Computational Biology Solutions using R and Bioconductor* 397–420 (Springer, 2005).

53.    Carlson, M., Falcon, S., Pages, H. & Li, N. hgu133plus2.db: Affymetrix Human Genome U133 Plus 2.0 Array annotation data (chip hgu133plus2). **R package version 2.6.3,**

## 8   Abbreviations

| | |
|---|---|
| % | percentage |
| µ | micro |
| 4E-ASO | eIF4E-antisense oligonucleotide |
| 4E-BP1 | eIF4E-binding protein |
| 4Ei-1 | eIF4e inhibitor-1 |
| 5' UTR | 5' untranslated region |
| 5-ALA | 5-aminolevulinic acid |
| APS | ammoniumpersulfate |
| BCPC | brain cancer-propagating cells |
| BSA | bovine serum albumin |
| CDK | cyclin-dependent kinase |
| CDKN2A | cyclin-dependent kinase inhibitor 2A |
| cDNA | complementary DNA |
| Ct | cross threshold |
| DEPC | Diethylpyrocarbonat |
| DMEM | Dulbecco's Modified Eagle's Medium |
| dNTP | deoxyribonucleosid triphosphate |
| EGFR | endothelial growth factor receptor |
| eIF | eukaryotic initiation factor |
| Erk | extracellular signal-regulated kinase |
| FBS | fetal bovine serum |
| Fwd. | forward |
| g | gram |
| GAPDH | glyceraldehyde 3-phosphate dehydrogenase |
| GBM | glioblastoma multiforme |
| GSC | glioma stem-like cell |
| GTP | guanosintriphosphate |
| h | hour |
| IDH1 | isocytrate dehydrogenase 1 |
| IHC | immunohistochemistry |

| | |
|---|---|
| l | liter |
| LOH | loss of heterozygosity |
| m7G cap | 7-methyl guanosine cap |
| MAPK | mitoge-activated protein kinase |
| *MDM2* | murine double minute oncogene |
| MEM | Minimum Essential Medium |
| Met-tRNAi | methionyl-tRNA |
| MGMT | $O^6$-methylguanine-DNA methyltransferase |
| ml | milliliter |
| mm | millimeter |
| mM | millimolar |
| mRNA | messenger ribonucleic acid |
| mTOR | mammalian target of rapamycin |
| NF1 | neurofibromin 1 |
| nm | nanometer |
| NP-40 | nonyl phenoxypolyethoxylethanol-40 |
| p70S6K | p70 ribosomal S6 kinase |
| PBS | phosphate buffered saline |
| PDCD4 | programmed cell death protein 4 |
| PDGFR | platelet-derived growth factor |
| PDGFRA | platelet-derived growth factor alpha |
| PI3K | phosphatidylinositol 3-kinase |
| PIK3CA | phosphatidylinositol 3-kinase catalytic subunit alpha |
| PIK3R1 | phosphatidylinositol 3-kinase regulatory subunit 1 |
| PTEN | phosphatase and tensin homolog deleted on chromosome 10 |
| PVDF | polyvinylidene difluoride |
| RAS | rat sarcoma protein |
| RB1 | retinoblastoma protein |
| REMBRANDT | Repository of Molecular Brain Neoplasia Data |
| Rev. | reverse |
| rpm | revolutions per minute |
| RT | room temperature |

| | |
|---|---|
| RTK | receptor tyrosine kinase |
| RT-PCR | reverse transcription-polymerase chain reaction |
| SDS-PAGE | sodium dodecyl sulfate polyacrylamide gel electrophoresis |
| shRNA | short hairpin RNA |
| TBS | Tris-buffered saline |
| TCGA | The Cancer Genome Atlas |
| TEMED | tetramethylethylenediamine |
| TIC | tumor-initiating cells |
| TIS | total immunostaining score |
| TP53 | tumor protein 53 |
| V | volt |
| VEGF | vascular endothelial growth factor |
| WHO | World Health Organization |

## 9 Acknowledgements